Tesis defendida por
Diego Luis Delgado Álvarez
y aprobada por el siguiente Comité

Dr. Salomón Bartnicki García
Director del Comité

Dra. Rosa Reyna Mouriño Pérez

Co-Directora del Comité

Dra. Meritxell Riquelme Pérez

Miembro del Comité

Dr. Brian D. Shaw

Miembro del Comité

Dr. Fernando Lara Rojas

Miembro del Comité

Dr. Fernando Díaz Herrera

Coordinador
del Posgrado en Ciencias de la Vida

Dr. Jesús Favela Vara

Director de la
Dirección de Estudios de Posgrado

Enero de 2014

CENTRO DE INVESTIGACIÓN CIENTÍFICA Y DE EDUCACIÓN SUPERIOR DE ENSENADA, BAJA CALIFORNIA

Programa de Posgrado en Ciencias
de la Vida con orientación de Microbiología

El citoesqueleto de actina en la endocitosis y el desarrollo de los septos en
Neurospora crassa

Tesis
para cubrir parcialmente los requisitos necesarios para obtener el grado de
Doctor en Ciencias

Presenta:

Diego Luis Delgado Álvarez

Ensenada, Baja California, México
2014

Resumen de la tesis de Diego Luis Delgado Álvarez, presentada como requisito parcial para la obtención del grado de Doctor en Ciencias en Ciencias de la Vida con orientación en Microbiología.

El citoesqueleto de actina en la endocitosis y el desarrollo de los septos en *Neurospora crassa*

Resumen aprobado por:

_____
Dr. Salomón Bartnicki García

La actina juega un papel esencial en una gran variedad de procesos celulares, que incluyen crecimiento celular, movilidad intracelular y citocinesis. La organización y dinámica de la F-actina fue visualizada mediante microscopía confocal y de campo evanescente en *Neurospora crassa* que expresaban fusiones a GFP o mChFP de proteínas como fimbrina y tropomiosina, dos subunidades del complejo Arp2/3 y el marcador global de F-actina, Lifeact. FIM-GFP, ARP-3-GFP, y Lifeact-GFP se asociaron a parches en la cara citosólica de la membrana celular, concentrados principalmente en un collar subapical. Estos parches eran de vida corta y mostraban varios grados de movilidad. TPM-1-GFP y Lifeact-GFP co-localizaban con el núcleo del Spitzenkörper y también se observaron decorando cables a lo largo de la hifa. También se determinó la dinámica de actina durante la formación del septo, asi como de la miosina clase 2 (Myo-2), tropomiosina, formina, fimbrina, BUD-4 y quitina sintasa 1 (CHS-1). Se reconocieron tres etapas de desarrollo del septo: 1) ensamblaje de la maraña de actomyosina (SAT) más de cinco minutos antes del crecimiento de la membrana plasmática, 2) formación del anillo contráctil de actomiosina (CAR), 3) constricción del CAR junto con el crecimiento centrípeto de la membrana plasmática y la formación de la pared celular del septo. Tropomiosina y Myo-2 fueron componentes del SAT que se condensa gradualmente hasta formar un proto-CAR. Durante su constricción, el CAR se asoció con el borde de la membrana en crecimiento. La formina y la BUD-4 se reclutaron durante la transición de SAT a CAR, y CHS-1 se detectó dos minutos antes que la constricción del CAR. Los parches de actina se asociaron a la membrana plasmática flanqueando el CAR. Estos resultados indican que cada estructura de F-actina se asocian a proteínas de unión a actina particulares que reflejan la función celular que desempeñan. El hecho de que Lifeact presente el mayor rango de marcaje de estructuras de F-actina sugiere que se trata de un marcador global de la F-actina. La regularidad espaciotemporal de la formación del septo puede indicar la integración de los mecanismos de control del ciclo celular y el crecimiento hifal.

Palabras clave**: Actina, Proteínas de unión a actina, formación del septo, Spk, endocitosis**

Abstract of the thesis presented by Diego Luis Delgado Álvarez as a partial requirement to obtain the Doctor of Sciences in Life Sciences degree in Microbiology.

The actin cytoskeleton during endocytosis and septum development in *Neurospora crassa*

Abstract approved by:

_____
Dr. Salomón Bartnicki García

Filamentous actin (F-actin) plays essential roles in filamentous fungi, as in all other eukaryotes, in a wide variety of cellular processes including cell growth, intracellular motility, and cytokinesis. We visualized F-actin organization and dynamics in living *Neurospora crassa* via confocal microscopy of growing hyphae expressing GFP fusions with homologues of the actin-binding proteins fimbrin (FIM) and tropomyosin (TPM-1), a subunit of the Arp2/3 complex (ARP-3) and a recently developed live cell F-actin marker, Lifeact (ABP140 of *S. cerevisiae*). FIM-GFP, ARP-3-GFP, and Lifeact-GFP associated with small patches in the cortical cytoplasm that were concentrated in a subapical ring, which appeared similar for all three markers but was broadest in hyphae expressing Lifeact-GFP. These cortical patches were short-lived, and a subset was mobile throughout the hypha, exhibiting both anterograde and retrograde motility. TPM-1-GFP and Lifeact-GFP co-localized within the Spitzenkörper (Spk) core at the hyphal apex, and were also observed in actin cables throughout the hypha. For septum formation we studied the dynamics of actin, myosin, tropomyosin, formin, fimbrin, BUD-4, and CHS-1. In chronological order, we recognized three septum development stages: 1) septal actomyosin tangle (SAT) assembly, 2) contractile actomyosin ring (CAR) formation, 3) CAR constriction together with plasma membrane ingrowth and cell wall construction. Septation begins with the assembly of a conspicuous tangle of cortical actin cables (SAT) in the septation site >5 min before plasma membrane ingrowth. Tropomyosin and myosin were components of the SAT. The SAT gradually condensed to form a proto-CAR preceding CAR formation. During its constriction, CAR was associated with the advancing edge of the growing septum. Formin and BUD-4 were recruited during the transition from SAT to CAR and CHS-1 was detected two min before CAR constriction. Actin patches associated to the septum membrane flanking the CAR. These results indicate that each F-actin structure is associated to particular F-Actin Binding Proteins reflecting the cellular function that they perform. The fact that Lifeact-GFP has the broadest spectrum of F-actin structure labeling suggests that it may serve as a global live cell marker for F-actin. The spatiotemporal regularity of septum formation could be indicative of the integrated mechanisms of cell cycle control and hyphal growth.

Keywords: **Actin, Actin Binding Proteins, septum formation, Spk, endocytosis**

Dedicatorias

Agradecimientos

Agradezco a todas las entidades que hicieron posible el desarrollo de mi tesis. Al CONACyT por el apoyo financiero mientras se pudo. Al CICESE por la hospitalidad institucional, incluyendo a todas las Divisiones, Despachos, Departamentos y Demás, en particular a la División de Biologia Experimental y Aplicada y en más particular aún, al Departamento de Microbiología por 7 años (incluyendo la Licenciatura) de sana diversión.

A los miembros del comité: Dra. Meritxell Riquelme, Dr. Brian Shaw, Dr. Fernando Lara. Y en penúltimo, último, y último final (ahora sí, v.10.1.2 FINAL), respectivamente, al Laboratorio Mouriño, al Dr. Salomón Bartnicki y a la Dra. Rosa Mouriño por los intensos períodos de retroalimentación intelectual.

Agradezco también a todos los amigos que hice dentro del CICESE y la Arizona State University, que (por fortuna) son muchos para mencionarlos a todos (por desgracia), pero destaco (en orden cronológico): Lucrecia Ramos, Olga Callejas, Robby Roberson, Rosa Ma. Ramírez, Ariana Román, Naidy Pinoncely, Mario Yáñez, Ramón Echauri, Rosa Angelina, Roxy Fajardo, Jovani Catalán, Leonora Martínez, Arianne Ramírez, Ricardo Reyes. (a los demás les informaré personalmente).

A todo aquel con quien tuve el honor de defender los colores de un mismo equipo (Pelicarrones, Balonazo en la cara, No somos balonazo en la cara, Sembradores, Pichiinguis, Childs, Cool, Mecamoeba, Fish Taco, Prionchis, etc.).

Index

Figure List

Table List

Chapter 1: Introduction

The importance of F-actin in tip growing cells was recognized in fungal hyphae (Hasek and Bartnicki-García, 1994; Heath et al., 2000; Bartnicki-García, 2002), in which growth and wall extension are mainly focused on a single site at the apex resulting in production of a tubular cell (Bartnicki-García and Lippman, 1977;). In recent years, many studies have reaffirmed the central importance of F-actin and associated proteins in growth and spatial regulation of organelles in tip-growing fungal cells (Harris and Momany, 2004; Virag and Griffiths, 2004; Harris et al., 2005; Upadhyay and Shaw, 2008). Studies designed to disrupt F-actin function using chemical agents such as cytochalasin and latrunculin B confirmed that a polymerized actin cytoskeleton is required for normal apical growth, hyphal tip shape, and polarized secretion in different fungal organisms (McGoldrick et al., 1995; Harris et al., 1997; Torralba et al., 1998; McDaniel and Roberson, 2000; Taheri-Talesh et al., 2008).

F-actin interacts with other proteins that regulate its arrangement and organization. In a wide variety of species studied, F-actin can be found as two main arrays: patches and cables, whose structure is dependent on the association of actin microfilaments to different Actin Binding Proteins (ABPs). Each of these arrays is responsible for a distinct actin-dependent process (Adams et al., 1991; Roberson, 1992; Arai et al., 1998; Sandrock et al., 1999; Pruyne and Bretscher, 2000; Bretscher, 2003; Moseley and Goode, 2006; Upadhyay and Shaw, 2008;

Taheri-Talesh et al., 2008). For example, tropomyosin stabilizes F-actin and regulates F-actin mechanics (Greenberg et al., 2007), Arp2/3 complex nucleates F-actin branches (Egile et al., 2005) and fimbrin cross-links F-actin into bundles and networks (de Arruda et al., 1990).

In filamentous fungi, actin visualized by various methods has been observed in the Spitzenkörper (Spk), a vesicle-rich area within the hyphal apical cytoplasm directly adjacent to the growth site (Howard, 1981; Roberson and Fuller, 1988; Bourett and Howard, 1991; Roberson, 1992; Srijayanthi et al., 1996; Virag and Griffiths, 2004; Harris et al., 2005; Upadhyay and Shaw, 2008; Taheri-Talesh et al., 2008). The population of F-actin in the Spk has been proposed to regulate vesicle delivery and/or fusion at the growth site (exocytosis), and may also regulate calcium channels, whose activity is important for tip growth (Hasek and Bartnicki-Garcia, 1994; Bartnicki-Garcia, 2002; Harris and Momany, 2004; Harris et al., 2005). Cortical F-actin patches have been proposed to play a role in plasma membrane invagination during endocytosis in filamentous fungi as well as yeasts (Mulholland et al., 1994; Harris and Momany, 2004; Ayscough, 2005; Rodal et al., 2005). In all fungi examined, F-actin patches are located at sites of active endocytic uptake (i.e., the subapex and septa) (Ayscough, 2005; Gachet and Hyams, 2005; Kaksonen et al., 2005; Upadhyay and Shaw, 2008; Taheri-Talesh et al., 2008).

Most studies of F-actin organization in filamentous fungi have used anti-actin antibodies or rhodamine phalloidin to label fixed cells. Filamentous actin is notoriously difficult to preserve during fixation and can often be difficult to

adequately label (e.g., phalloidin is usable for only a small number of fungal species). Thus, some of the differences previously described in studies with different fungi may be caused by fixation artifacts or the source of anti-actin antibodies (Heath et al., 2000; Virag and Griffith, 2004). Recently, live cell imaging of F-actin has been done in *Aspergillus nidulans* germlings using green fluorescent protein (GFP) fused to G-actin and to different ABPs such as fimbrin and tropomyosin (Upadhyay and Shaw, 2008; Taheri-Talesh et al., 2008).

Another F-actin-dependent process important for fungal development is septum formation. These cells are compartmentalized by cross walls that retain a central pore through which cytoplasm and organelles including nuclei flow freely. The controlled segmentation of hyphal units is the basis for the morphological complexity achieved by septated fungi (Gull, 1978; Harris, 2011). Moreover, septa may provide structural integrity to the hyphal tube, preventing cytoplasmic leakage of the entire colony by plugging the septal pore with Woronin bodies when the tube is injured (Bracker, 1967; Gull, 1978; Gregory, 1984; Fleissner et al., 2005; Jedd and Chua, 2000; Liu et al., 2008). Nevertheless, hyphal septa are not essential, since groups of fungi do well without them. However, mutants of *N. crassa* lacking septa display cytoplasmic leakage and are deficient in conidiation (Rasmussen and Glass, 2005; Justa-Schuch et al., 2010). The vegetative mycelium is composed of multinucleated cells divided by regularly spaced septa. Septa construction requires regulation of mitosis, cytokinesis and cell wall biosynthesis (Momany et al., 1995). During septum formation, a conserved set of proteins follow a similar temporal and spatial pathway in different eukaryotes to assemble F-actin-containing structures

that contribute to septation (Bezanilla et al., 2000; Paoletti and Chang 2000; Wong et al., 2002; Motegi et al., 2000, 2004). It is well established that the actin-based contractile ring functions in membrane contraction during septation, but the role of actin patches is less clear. The Arp2/3 complex is found in F-actin patches flanking the contractile ring in *Schizosaccharomyces pombe* (McCollum et al., 1996; Arai et al., 1998; Morell et al., 1999; Wu et al., 2006). These patches are thought to promote endocytic uptake required for cytokinesis in *S. pombe*, although the Arp2/3 complex is not required for cytokinesis in *Drosophila melanogaster* (Eggert et al., 2004).

Hyphal septation resembles the one in yeast cells but without the final step of cell separation. These two processes share key features such as the selection of the cross wall formation site, the assembly of a contractile actomyosin ring (CAR) and the coupled processes of plasma membrane ingrowth and cell wall construction (Chant and Pringle, 1991; Bulawa 1993; Momany; Beck *et al.*, 1995; Seiler and Justa-Schuch, 2010; Mouriño-Pérez, 2013, Mouriño-Pérez and Riquelme, 2013). In contrast to unicellular yeasts, in filamentous fungi each nuclear division may or may not be coupled with a round of cytokinesis. The lack of coupling, e.g. in *N. crassa*, produces multinucleated hyphal compartments. In other fungi, e.g. *A. nidulans,* CAR assembly and septum formation is clearly controlled through nuclear position and cell cycle progression (Harris *et al.* 1994; Wolkow *et al.* 1996; Momany and Hamer 1997a, 1997b; Harris; 2001). Although a correlation between mitosis and septation may exist in *N. crassa* (Serna and Stadler, 1978; Minke *et al.*, 1999; Plamann *et al.*, 1994; Gladfelter, 2006, Riquelme *et al.*, 2011),

the asynchronous mitosis in this fungus makes the connection between cell cycle and septum formation difficult to establish.

Hyphae are compartmentalized with precision, suggesting that septum initiation is a well-regulated event (Harris, 2001). However, the mechanism for determining the septation site of septum formation differs between organisms belonging to the same phylum. Budding and fission yeast, for example, have developed fundamentally distinct mechanisms to ensure proper nuclear segregation. The site of bud emergence in *S. cerevisiae* uses cortical cues from the previous cell division cycle, while in *S. pombe*, opposing nuclear and cell end-dependent spatial signals are integrated in order to trigger medial cell division (Chang and Peter 2003; Seiler and Justa-Schuch, 2010). However, in both cases cortical anillin-like landmark proteins and a kinase cascade called septation initiation network (SIN) are critical for selection of the division site, temporal-spatial organization of the CAR and coordination of cell cycle progression with CAR constriction (Park and Bi, 2007; Martin, 2009). The homologs of the *S. cerevisiae* axial bud site marker proteins, Bud3p and Bud4p, are important for septum formation in *N. crassa* and *A. nidulans* (Justa-Schuch *et al.* 2010; Si *et al.*, 2010; Si *et al.*, 2012). In *N. crassa*, both proteins appear prior to the formation of a detectable septum as cortical rings at incipient septation sites that contract with the forming septum (Justa-Schuch *et al.* 2010).

This study was focused on visualization of the F-actin cytoskeleton in living mature hyphae of *N. crassa* in order to describe its dynamics and organization during hyphal growth and septum formation using different

microscopy techniques. Several ABPs, such as tropomyosin, Arp2/3 complex and fimbrin all fused to GFP and a recently developed live cell F-actin reporter called Lifeact (Riedl et al., 2008) were analyzed. By a detailed characterization of the time of appearance of key proteins involved in septum formation we were able to determine the chronology of events during septum development in *N. crassa*. Our observations indicate that the assembly of a broad meshwork of long actomyosin cables, that we named the septal actomyosin tangle (SAT), is the first evidence of septum initiation. This SAT structure becomes compacted to form a tight ring, the CAR. Contrary to the claims of others (Berepiki et al., 2011), we determined that BNI-1, the only formin in *N. crassa*, and the landmark protein BUD-4 enter the septation process only at later stages during the transition of the SAT to the mature CAR.

.

Chapter 2: Goals and hypotheses

2.1 General goal

Describe the localization and dynamics of the components of the actin cytoskeleton in live mature hyphae of *Neurospora crassa* during apical growth and septum formation.

2.2 Specific goals

- Develop *N. crassa* strains expressing actin binding proteins (ABPs) fused to GFP and/or mChFP to document the presence and dynamics of these proteins in vivo.

- Determine the cellular localization of F-actin sub-populations associated with each of the different ABPs

- Determine the chronology of events leading to septum formation.

- Establish the correlation between confocal and electron microscopy images of ABPs involved in endocytosis.

2.3 Hypotheses

- Complete and truncated Actin Binding Domains (ABDs) of Actin Binding Proteins (ABPs) fused to GFP are reliable reporters of the actin cytoskeleton in *N. crassa*.
- Distinct ABPs are associated to different actin higher order structures.
- Actin is the first protein to target putative septation sites.

Chapter 3: Materials and methods

3.1 Strains and culture conditions

Strains used in this study are listed in Table 1 A. Strains were maintained on Vogel's minimal medium (VMM) with 2% sucrose. All manipulations were according to standard techniques (Davis, 2000).

3.2 Construction of GFP-containing plasmids

Standard PCR and cloning procedures (Sambrook et al., 1989) were used to fuse the *sgfp* gene to the carboxyl terminus of *fim*, abd1, abd2, (truncated version of fimbrin), *arp-2*, *arp-3* and *tpm-1*. Truncated versions of fimbrin each one contained one actin-binding domain (abd1 or abd2) (Fig. 1) (Wang et al., 1998). All the genes and truncated versions of fimbrin were amplified by PCR from *N. crassa* (FGSC 2489) genomic DNA. Primers used are listed in Table 1 B. PCR was performed in a Bio-Rad Thermal Cycler with Platinum Hi-fi *Taq* polymerase (Invitrogen, Carlsbald, CA) according to the manufacturer's instructions. The amplified and gel-purified PCR products were digested with *Xba*I and *Pac*I and ligated into *Xba*I- and *Pac*I-digested plasmid pMF272 (GenBank accession no. AY598428). This yielded pRM08-DD01 (*fim*), pRM11-DD02 (abd1), pRM10-DD03 (abd2) and pRM47-OC28 (*tpm-1*) (Table 1 C).

Table 1. Materials used. (A) *N. crassa* strains, (B) plasmids and (C) oligonucleotides.

	Genotype, description, or sequence	Reference
(A) Strains		
Wild type 2489	*mat a*	FGSC2489
9717	*mat A his-3; Δmus-51::bar⁺*	FGSC9717
dRFP-TPM	*mat a his-3⁺::Pccg-1-drfp-tpm-1*	1
TRM47-OC28	*mat a his-3⁺::Pccg-1-tpm-1-sgfp⁺*	1
TRM08-DD02	*mat a his-3⁺::Pccg-1-fim-1-sgfp⁺*	1
TRM10-DD04	*mat a his-3⁺::Pccg-1-fim-1 (abd1)-sgfp⁺*	1
TRM11-DD05	*mat a his-3⁺::Pccg-1-fim-1 (abd2)-sgfp⁺*	1
TLS-NG01	*mat a his-3⁺::Parp2-arp-2-sgfp⁺*	1
TLS-NG02	*mat a his-3⁺::Pccg-1-arp-3-sgfp⁺*	1
TRM49-OC30	*mat a his-3⁺::Pccg-1-lifeact-egfp⁺*	1
bni-1-sgfp	*bni-1Δ::hph his-3+::Pccg-1-bni-1-sgfp*	2
bud-4-gfp	*bud-4Δ::hph his-3+::Pccg-1-bud-4-sgfp*	2
chs-1-gfp	*mat A his-3+::Pccg-1::chs-1::sgfp+*	3
(B) Oligonucleotides		
FimF	**GCTCTAGA**ATGAATGTCCTCAAGATCCAG	1
FimR	**CCTTAATTAA**CTGCATCTTGTCATAGGTAGCCAT	1
Abd1F	**CTCTAGA**ATGTTCTTGAAGGCCACCCAGGTC	1
Abd1R	**CCTTAATTAA**GGCCAGTTGGCGGCCTTG	1
Abd2F	**CTCTAGA**ATGGAGAAGCTTGAGGTCGAG	1
Abd2R	**CCTTAATTAA**CTACTGCATCTTGTCATAGGT	1
TropF	**GCTCTAGA**ATGGACCGCATCAAGGAG	1
TropR	**CCTTAATTAA**GATGTTGGCAATATCAGCCT	1
Arp2F	**ACTAGT**TGATTGGTTCTTGCTGGGCG	1
Arp2R	**GGATCC**CAGCCCTAGGACCCAACTTCTCCAACAC	1
Arp3F	**TCTAGA**ACTAGTCAGCACACCACCGCAACAAT	1
Arp3R	**GGATCC**CAGCAGATCCACCAGGTCCTCCG	1
LifactF	GGG**TCTAGA**ATGGGTGTCGCAGATTTGAT	1
LifactR	CAC**GGGCCC**TTACTTGTACAGCTCGTCC	1
(C) Plasmids		
pMF272	*Pccg-1-sgfp⁺*	4
pRM47-OC28	*Pccg-1-tpm-1-sgfp⁺*	1
pRM08-DD02	*Pccg-1-fim-1-sgfp⁺*	1
pRM10-DD04	*Pccg-1-fim-1 (abd1)-sgfp⁺*	1
pRM11-DD05	*Pccg-1-fim(abd2)-sgfp⁺*	1
pRM49-OC30	*Pccg-1-lifeact-egfp⁺*	1
pLS-NG01	*Pccg-1-arp-2-sgfp⁺*	1
pLS-NG02	*Parp-2-arp-2-sgfp⁺*	1
pLS-NG03	*Pccg-1-arp-3-sgfp⁺*	1

*Restriction enzymes sequence in bold
References: ¹Delgado-Álvarez et al., 2010, ²Justa-Schuch et al., 2010, ³Sánchez-León et al., 2011, ⁴Freitag et al., 2007.

Only those without changes to the amino acid sequence were used in this study. *N. crassa* transformed with the Abd1-GFP construct showed no specific localization of GFP and was not examined further.

The *arp-3* gene amplified was digested with *Xba*I and *Bam*HI and cloned into *Xba*I- and *Bam*HI-digested pMF272 giving rise to the pLS-NG02 (*arp3*) (Table 1 C). The *arp-2* coding region and 943 nucleotides of sequence upstream of the ATG were amplified, digested with *Spe*I and *Bam*HI and ligated into a *Spe*I- and *Bam*HI-digested pMF272 lacking the *ccg-1* promoter producing the pLS-NG01 (*arp-2*) (Table 1 C). To create this derivative, pMF272 was digested with *Not*I and *Xba*I, ends were filled in with Klenow, and the larger fragment was self-ligated. In *arp-2* and *arp-3* constructs, vector-derived sequences encode an 8 aminoacid linker (AGIPGLIN) separating the last amino acid of ARP-2 or ARP-3 from the first amino acid of GFP (Egile et al., 2005).

The first 17 aa (MGVADLIKKFESISKEE) of Abp140 of *S. cerevisiae* were shown to label F-actin comparable to the full-length protein. This small peptide named 'Lifeact' is conserved among many fungal species and it is a good F-actin marker for higher eukaryotes (Riedl et al., 2008). Lifeact sequence was cloned into pMF272 as a C-terminal GFP fusion (Lifeact-GFP) with the aminoacids GDPPVAT between the last aminoacid from Lifeact and the first aminoacid from GFP. The Lifeact-linker-*egfp* was amplified by PCR and digested with *Xba*I and *Apa*I and ligated into *Xba*I- and *Apa*I-digested pMF272,, removing the *sgfp* sequence in the plasmid. This yielded pRM49-OC30 (Lifeact-*gfp*). All constructs were sequenced at Eton Biosciences (San Diego, CA).

3.3 Transformation protocols, selection of transformed strains and crosses

Transformation of *N. crassa* strain FGSC9717 *Δmus-51 his-3* conidia with non-linearized plasmids (Table 1) was carried out by electroporation on a Bio-Rad Gene Pulser (capacitance, 25 µF; 1.5 kV; resistance, 600 Ω) as previously described. Prototrophic *his+* transformants were screened for the expression of GFP by epifluorescence microscopy as described previously (Freitag et al., 2004). Transformants showing strong fluorescence were selected. The heterokaryon strain selected of each transformation was crossed to the homokaryotic strain *mat a* (FGSC2489). Strains were crossed routinely on Petri plates with synthetic crossing medium (SCM) supplemented with 1% sucrose and 2% agar (Davis, 2000).

3.4 Double labeling

To observe the relationship between ABPs we constructed two heterokaryons from three *N. crassa* strains, one with the Lifeact-GFP and TPM-1-mchFP and the other with Abd2-GFP and TPM-1-mchFP. A Petri plate with VMM was inoculated with mycelia from each pair of strains and incubated for 12 h at 30ºC. The margin of the colonies was screened for hyphae having both fluorescent makers and then imaged following the procedure described for laser scanning confocal microscopy.

3.5 F-actin and microtubules depolymerization assays.

Stock solutions of cytochalasin A (Cyt A) (Sigma–Aldrich, St. Louis, Mo), latrunculin A (Lat A) (anti-actin drugs) and benomyl (anti-microtubules drug) (Sigma–Aldrich) at 10 mg ml^{-1} were prepared in 100% ethanol. The concentration that inhibited the hyphal growth rate by 50% was selected from Ramos-García et al. (2009) for further studies. To study the effect of Cyt A and Lat A on the distribution of ABPs in *N. crassa*, we exposed the cells to 1 µg ml^{-1} of Cyt A and 20 µg ml^{-1} of Lat A diluted in VMM broth. A drop of 50 µl of the solution was placed on a coverslip; a block of agar (Hickey et al., 2002) containing *N. crassa* mycelium was placed on the inhibitor solution, and after 5-10 minutes of exposure the cells were imaged. For benomyl experiments, we inoculated VMM plates amended with 2.5 µg ml^{-1} and incubated at 28ºC until the cells reached a young mycelium stage (~16 h). For all treatments, mycelia were observed following the procedure described for laser scanning confocal microscopy (see below).

3.6 Laser scanning confocal microscopy of living cells

Strains containing *arp-2*::*sgpf*, *arp-3::sgfp, fim-1::sgfp, myo-2::gfp tpm-1::sgfp*, *bud-4::sgfp*, *bni-1::sgfp*, *chs-1::sgfp* and *Lifeact::egfp* were grown on VMM. The "inverted agar block" method (Hickey et al., 2002) was used for live-cell imaging with an inverted laser scanning microscope (LSM-510 Meta, Carl Zeiss, Göttingen, Germany) equipped with an argon ion laser for excitation at 488nm wavelength and GFP filters for emission at 515–530 nm. An oil immersion objective was used:100x (PH3)/1.3 N.A. Laser intensity was kept to a minimum (1.5%) to

reduce photobleaching and phototoxic effects. Time-lapse imaging was performed at scan intervals of 0.5 to 4.5 s for periods up to 40 min. Image resolution was 512 ✕ 512 pixels and 300 dpi. Confocal images were captured using LSM-510 software (version 3.2; Carl Zeiss) and evaluated with an LSM 510 Image Examiner. Some of the image series were converted into movies (*.mov) using the same software. Time-lapse images of hyphae were recorded simultaneously by phase contrast microscopy and fluorescent confocal microscopy. Phase contrast images were captured with a photomultiplier for transmitted light using the same laser illumination for fluorescence (Mouriño-Pérez et al., 2006). Some of the image series were converted into movies (*.mpeg) using AVS Video Converter v8.1 (Online Media Technologies LTD.). Final images were processed, and figures were created using Adobe Photoshop CS5 Extended and Adobe Illustrator CS5 (Adobe Systems Inc., San Jose, CA) and SketchUp (Google[TM]).

3.7 TIRF (Total Internal Reflection Fluorescence Microscopy)

Total Internal Reflection Fluorescence Microscopy (TIRFM) selectively illuminates and excites fluorophores in a restricted region of the specimen immediately adjacent to the glass-sample interface through an evanescent wave that is generated when the incident light is totally reflected at the glass-sample interface. The evanescent electromagnetic field penetrates to a depth of only approximately 100 nm into the sample medium. Thus, the TIRFM enables a selective visualization of surface regions such as the basal plasma membrane (Axelrod, 2001; Steyer and Almers, 2001).

For TIRFM, an IX-70 inverted microscope equipped with a 60x/1.45 N. A. Apochromat objective lens (Olympus Corp., Melville, NY) and a krypton/argon laser (Melles Griot, Carlsbad, CA) (488 nm) was used. Images were recorded with a Cascade 512B EMCCD camera (Photometrics, Tucson, AZ) for durations of 2-3 min at 512 × 512 resolution and frame rates of 50-100 msec. MetaMorph 6.0/6.1 software (Universal Imaging, Downingtown, PA) was used to control the camera and capture images. Final images were processed, and figures were created with Adobe Photoshop CS3 Extended (Adobe Systems Inc.).

3.8 Membrane Fluorescent staining

Using the ''inverted agar block method'' for preparing and staining samples (Hickey et al., 2002), GFP-expressing strains were incubated with 2.5 µM FM4-64 (Molecular Probes, Eugene, OR), which labels the plasma membrane and organelle membranes (Fischer-Parton et al., 2000).

3.9 Definition of hyphal regions

Hyphal regions were defined previously (McDaniel and Roberson). Region I contains the Spk, Region II extends from the posterior side of the Spk to the anterior side of the first nucleus, and Region III extends over a variable distance from the anterior side of the first nucleus to a zone characterized by the presence of large vacuoles.

3.10 Imaging of the Septation Initiation Site (SIS)

In order to capture the events prior to septum formation, 95 µm were measured from the last formed septum towards the tip. Then, a time series was started.

3.11 GFP-Immunoelectron Transmission Microscopy

3.11.1 Dialysis membrane preparation.

Dialysis membranes were first boiled in distilled and deionized water for 2 days to remove salts and then sterilized at 121ºC and 15 psi for 15 minutes and stored at 4 ºC for future use.

3.11.2 Cryofixation chamber.

The cryofixation chamber consists of two hollow and concentric cylinders. The space between (aprox. 5 cm) was filled with liquid nitrogen (-196 ºC). The internal cylinder (the Cryofixation Chamber, properly) was then filled with gaseous propane. Propane condensed into liquid when it made contact with the metal walls of the CCh. Liquid propane was constantly homogenized to ensure a continuous temperature. Cryule vials were placed inside the CCh after plunging the membranes.

3.11.3 Primary and secondary antibodies.

Rabbit-raised primary antibodies (Ab) (anti-GFP) were obtained from Abcam®. According to the manufacturers site "this antibody is reactive against all

variants of *Aequorea victoria* GFP such as S65T-GFP, RS-GFP, YFP and EGFP. It was also shown to work with AcGFP. For WB, IP-WB and ICC/IF" (http://www.abcam.com/gfp-antibody-ab290.html, 2012). The optimal dilution for effective labeling was 1:250. This dilution is used in all the results referenced here fore. Secondary Ab (anti-rabbit Fc) coupled to gold nanoparticles (10 nm in diameter) was obtained from the stock of the ASU SOLS imaging facilities (David Lowry). These Ab were used at a final dilution of 1:100.

3.11.4 Culture.

The ARP-2-GFP (*parp-2::gfp)* expressing *N. crassa* strain was inoculated on a dialysis membrane over MMV-agar and incubated first at 30 ºC for 4 h, then at RT for 1 h.

3.11.5 Membrane cutting.

The dialysis membrane containing the mycelium growing edge was cut with a razor blade. A small incision in he top right corner was made for future positional reference. Sectioned membranes were left on MMV-agar at RT for 1 h.

3.11.6 Cryofixation, chemical fixation and infiltration.

Membranes were plunge-frozen in propanol and then transferred to vials containing the fixing solution (Uranyl acetate 0.1%/Glutaraldehyde 0.2% in acetone) and incubated at -86 ºC for 3 days. Membranes were first washed 3 times (15 minutes each) with absolute ethanol at -20 ºC and then infiltrated for 2 h with

50% LR-Gold in ethanol. 50% LR-Gold/ethanol was removed and 100% LR-Gold was added. The membranes were incubated at -20 ⁰C overnight in a rotator.

3.11.7 Polymerization.

LR-Gold was removed and LR-Gold + initiator (benzoyl peroxide and benzoin methyl ether) was added. The membranes were incubated for 1 h at -20⁰C and then spread over a glass slide coated with Teflon® with the mycelium facing away from the glass slide. The slides with the membranes were covered with Aclar® film and then degased in a vacuum chamber. The slides were incubated in a polymerization chamber at -21⁰C for 24 h and then at RT for 4 h.

3.11.8 Cell selection and nanosectioning.

The criterion for selection of well-preserved cells was that they had a similar appearance to live cells and that they did not present freeze damage by light microscopy. Circles were engraved on the resin with a diamond knife. The resin was cut and glued to an epoxy-resin column. The region containing the cell was shaped like a trapezoid and thick-sectioned until the cell was close to surface of the column. The column was sectioned into 70 nm thick sections. Sections were recovered with polyvinyl formal (Formvar®) precoated gold grids.

3.11.8 Immunolabeling and post-staining.

The grids containing the cell sections were floated on a BL buffer drop at 4 ⁰C for 1 h for blocking unspecific epitopes. Then, excess BL buffer was removed

with a filter paper and the grids were floated on a drop of primary Ab diluted in BL buffer and incubated at RT for 1 h. The grids were washed three times (15 m each) and placed on a drop of secondary Ab solution. The grids were incubated at RT for 1 h and then washed three times. The grids were finally washed with ultra-pure H_2O and stored for future use. The sections were post-stained by floating the grids on a drop of 0.1 % uranyl acetate in water at RT for 5 m. Then, they were washed 3 times by immersion in ultra-pure water.

3.11.9 Transmission Electron Microscopy.

Transmission Electron Microscopy was performed on two different microscopes: a **Philips CM 12 TEM** fitted with a Gatan model 791 CCD camera for direct digital image acquisition and a **JEOL 1200EX TEM** fitted with a SIA L3C digital camera.

Chapter 4: Results

4.1 The Actin Cytoskeleton Of **Neurospora crassa**

4.1.1 Development Of F-Actin Reporters

To visualize F-actin in live cells of *N. crassa*, Actin Binding Proteins (ABPs) were fused to fluorescent proteins (GFP and/or ChFP) as reporters: Tropomyosin (TPM-1), ARP-2 and ARP-3 (Arp2/3 complex) and two Fimbrin-based constructs (FIM and ABD2) (Delgado-Álvarez, 2008). Also, the novel F-actin reporter Lifeact, was used. Lifeact consists of the first 17 aa of Abp140 of *S. cerevisiae* fused to the N-terminus of *egfp*) (Riedl et al., 2008). The *ccg-1* promoter drives the expression of Tropomyosin (TPM-1), ARP-2, and ARP-3, fused to GFP (Fig. 1). Additionally, an ARP-2 construct driven by its endogenous promoter was tested. The fluorescence intensity and the distribution of both ARP2-GFP constructs (driven by *pccg-1* and *parp-2*) and ARP-3-GFP was the same. Thus, we focused on the ARP-3-GFP marker for the studies reported in this section (Fig. 1). Tropomyosin (TPM-1-GFP and TPM-1-ChFP) decorates actin cables, Fimbrin (FIM-GFP) and ARP-2/3-GFP actin patches, and Lifeact labels both type of actin structures.
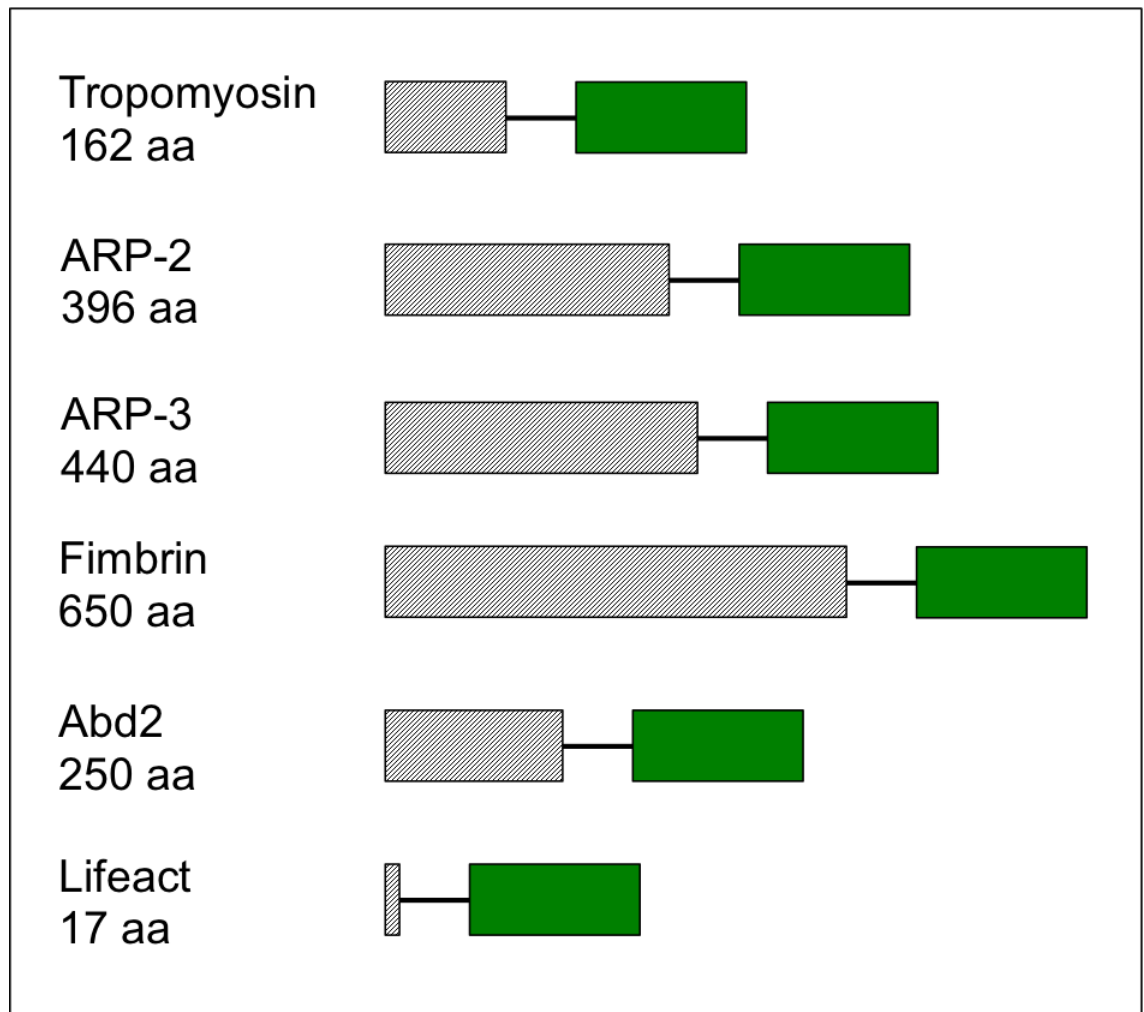
Figure 1: Schematic representation of the tropomyosin, Arp2/3, Fimbrin and Lifeact reporters. The grey boxes represent the protein/peptide aminoacid length and the green boxes represent the GFP protein.

4.1.2 The Actin Cytoskeleton In The Apex And Subapex Of Mature Hyphae

Tropomyosin associated with actin was present in the Spitzenkörper. All throughout polarized apical growth, Lifeact, TPM-1-GFP and TPM-1-ChFP (Fig. 2, Movie 1) co-localized with the Spitzenkörper (stained by FM4-64). Both Lifeact and

TPM-1-GFP were present in the core as a spherical-shaped aggregation. TPM-1-GFP was a sphere 1.5 ± 0.4 µm (mean ± standard error) in diameter occupying ~80% of the total area of the Spitzenkörper (Fig. 3A). Lifeact formed a sphere of 1.5 ± 0.6 µm in diameter (Fig. 3B).
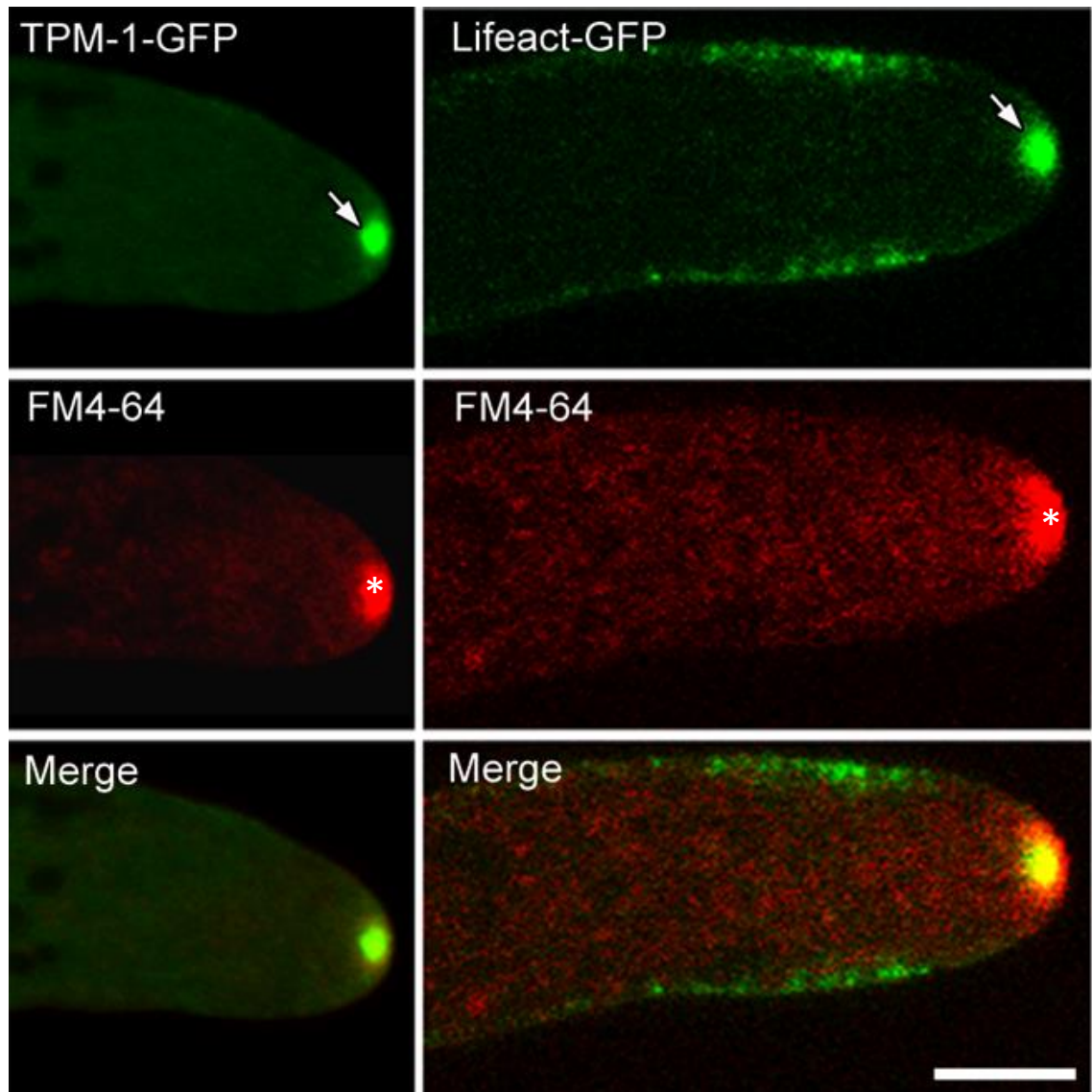
Figure 2: Actin is located in the core of the Spitzenkörper. Confocal imaging of growing hyphal tips expressing the actin reporters Tropomyosin and Lifeact (top panels). Vesicles in the Spitzenkörper are stained red with FM4-

64 (middle panels). Actin co-localizes with the core region of the Spitzenkörper (yellow, bottom panel). Scale bar = 5 µm.
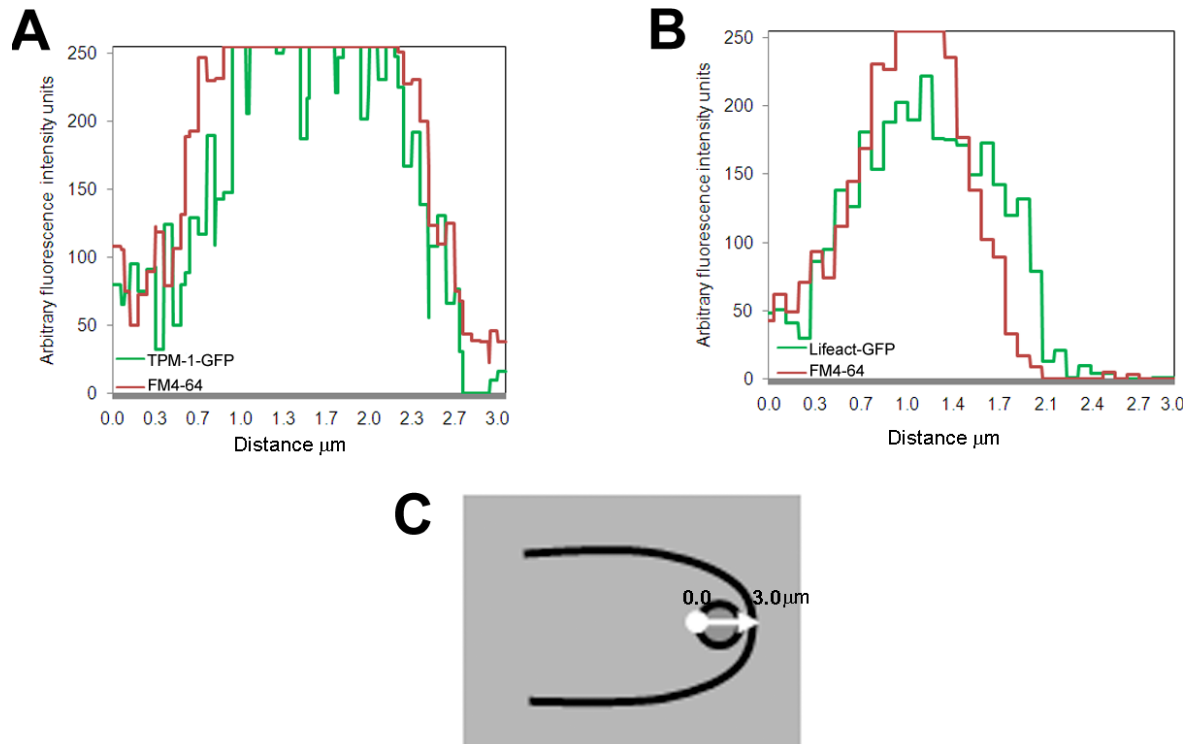
Figure 3: Fluorescence intensity plots of Tropomyosin-GFP (TPM-1-GFP) (A) and Lifeact (B) in the Spitzenkörper labeled with FM4-64. The Spk area plotted is represented in (C).

The co-expression of Lifeact and TPM-1-mChFP in fused hyphae revealed that TPM-1-mChFP co-localized to the center of the Lifeact accumulation (Fig. 4). The dynamics of both reporters mirrored the behavior of the Spitzenkörper (Movies 2 and 3).
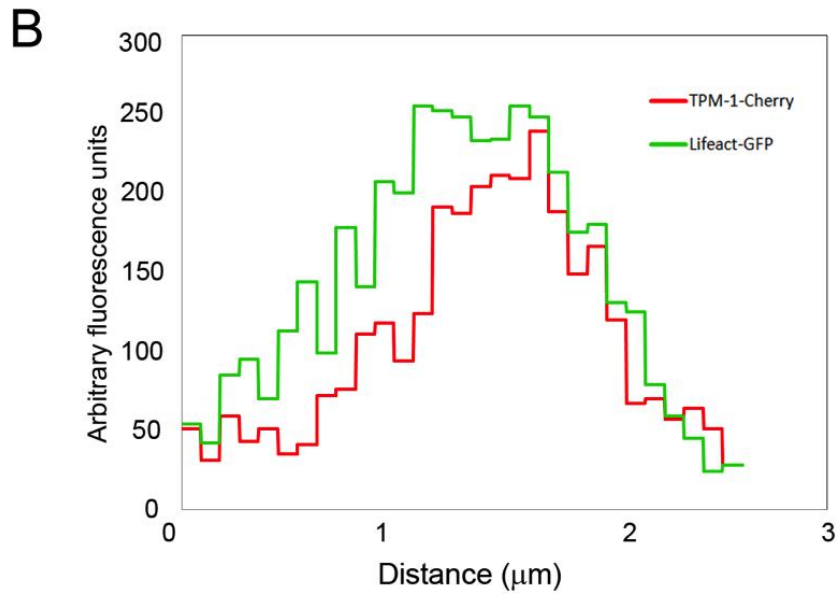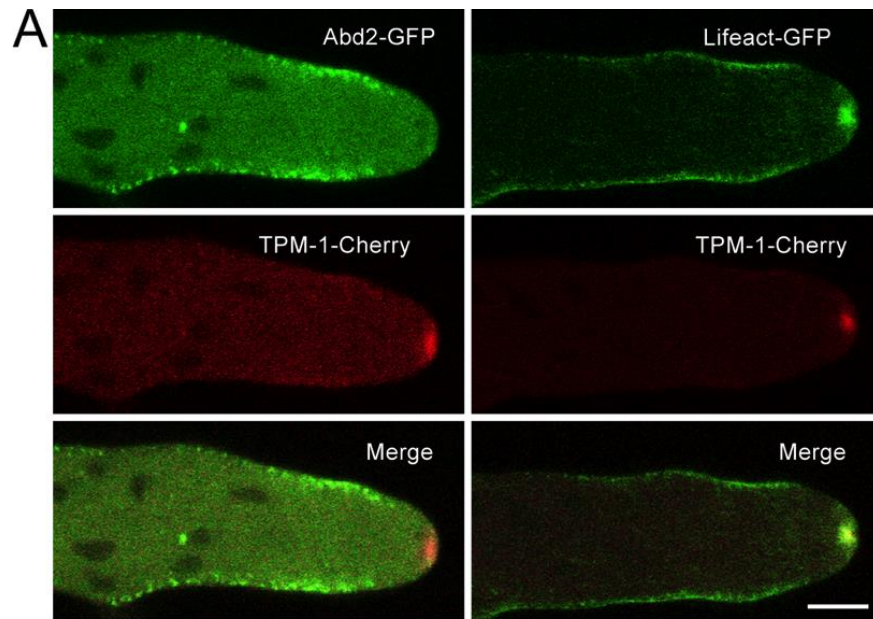
Figure 4: Actin patches are located in the hyphal subapex. Actin patches labeled by Fimbrin (Abd2-GFP; left panel in A) and Lifeact (right panel in B) are absent from the apical region.

4.1.3 Actin forms subapical patches and cortical cables

In the subapical region, members of the Arp2/3 complex were present as small cortical patches (0.5 µm ± 0.1, n=100) that aggregated to form a collar indistinguishable from FIM-GFP and ABD2-GFP (Delgado-Álvarez, 2008). The Arp2/3 and Lifeact patches appeared to co-localize with the cytosolic face of the plasma membrane stained with FM4-64 in identical fashion to FIM-GFP and ABD2-GFP patches (Figs. 2, 4 and 5. Movie 4). The subapical actin-patch collar started at $\sim$ 4.2-4.5 µm from the apex. The Lifeact collar had the greatest apparent width (21.3 ± 1.6 µm; n=60) (Fig. 6).

Actin cables were interspersed within the subapical collar and extended to the distal regions of the hyphae. TPM-1-GFP and Lifeact formed long and thin cable-like structures in the cell cortex arranged parallel to the longitudinal axis of the hypha (Fig. 7). Lifeact patches were often closely associated with these cables (see below *Actin patches are mobile*). Actin patches were present in a lower density in the basal region of hyphae compared to the subapex.
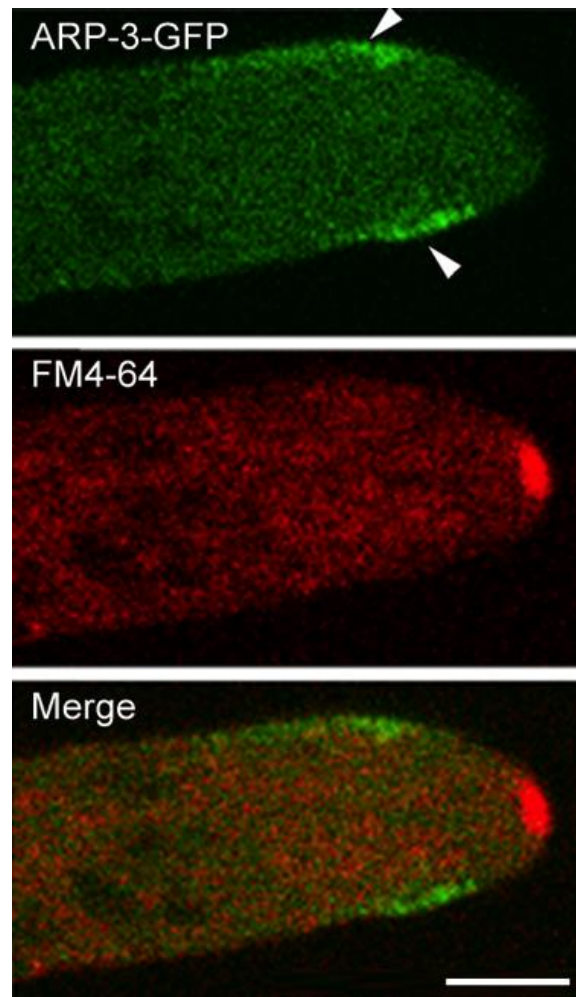
Figure 5: The Arp2/3 complex is located exclusively in actin patches. The subapical actin-patch collar (arrowheads) is labeled by the Arp2/3 complex. Scale bar = 5 μm
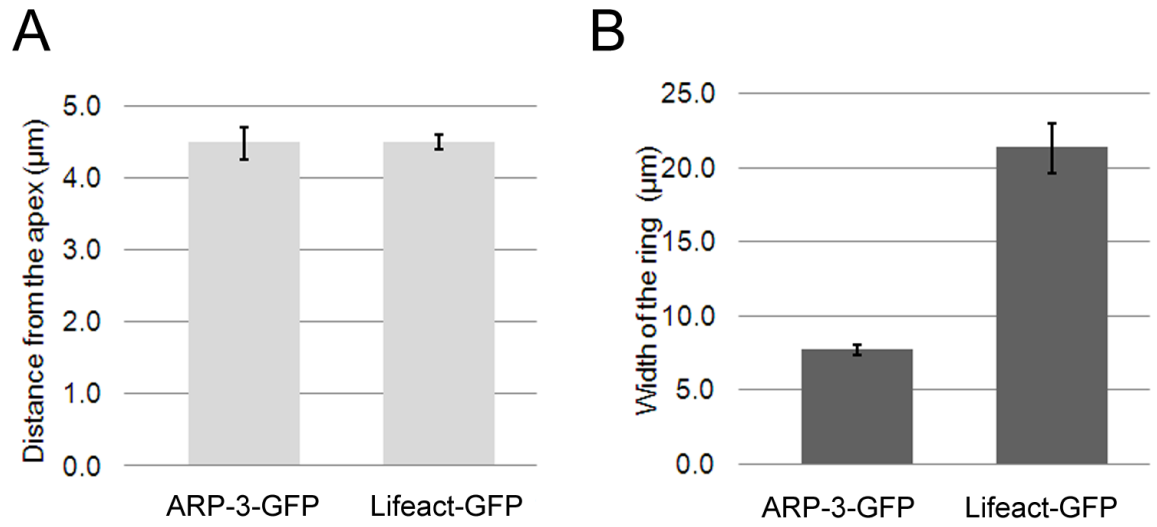
Figure 6: Actin patch collar is at a fixed distance from the apex. (A) Distance from the apex to the anterior edge of the subapical collar. (B) Subapical collar width.
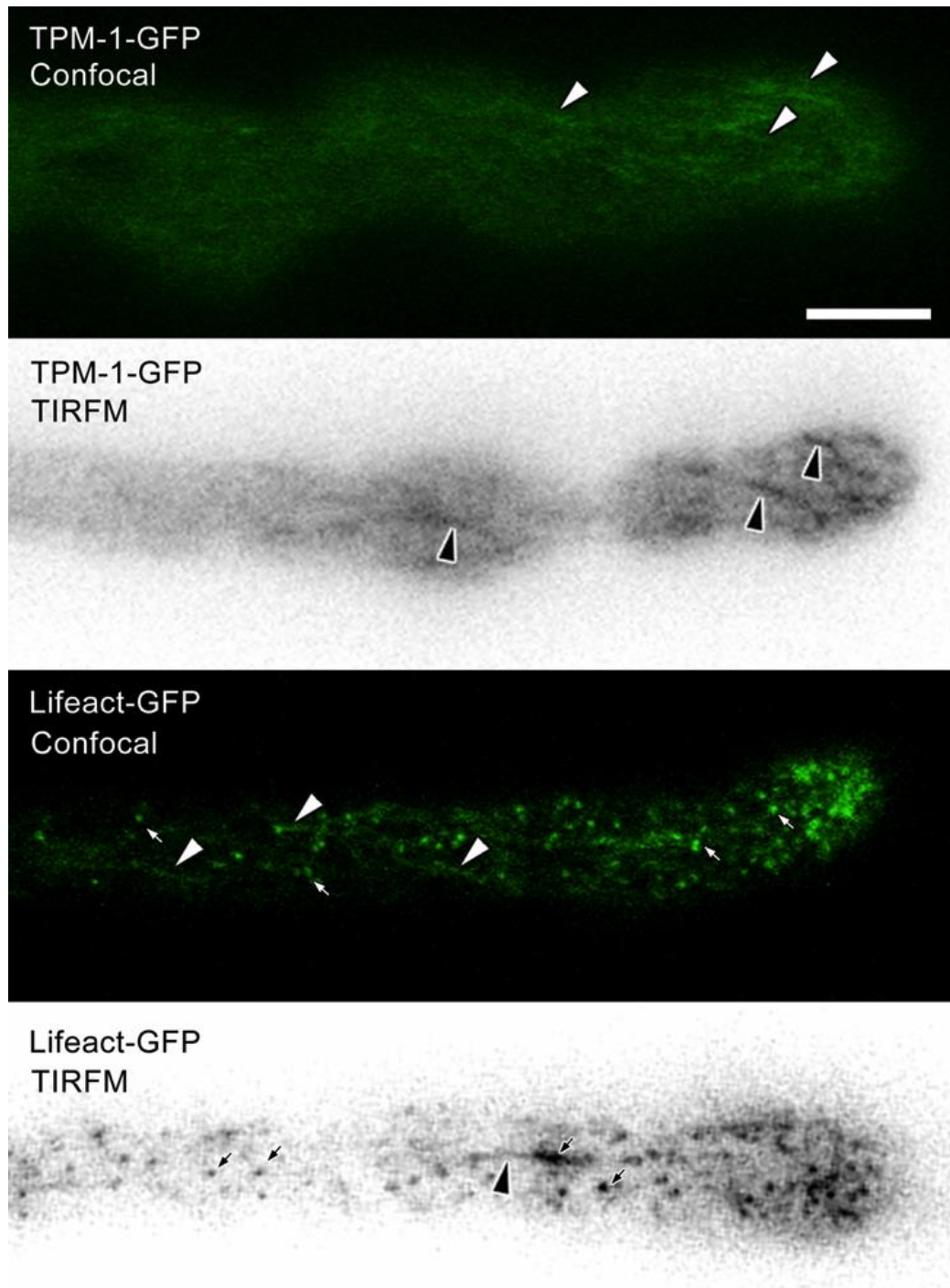
Figure 7: Actin forms cortical cables. Confocal and Total Internal Reflection Fluorescence Microscopy (TIRFM) imaging of actin cables labeled by Tropomyosin and Lifeact. Arrowheads show cables in both strains; arrows point to patches in the Lifeact strain. Scale bar = 5 μm.

The patch collar kept a constant distance from the apex during normal hyphal elongation, except when the Spitzenkörper disassembled and hyphal extension stopped. In these cases, the subapical collar lost its localization, the tip swelled and the patches reached the hyphal tip. As growth resumed, the collar was once again positioned subapically (Fig. 8).
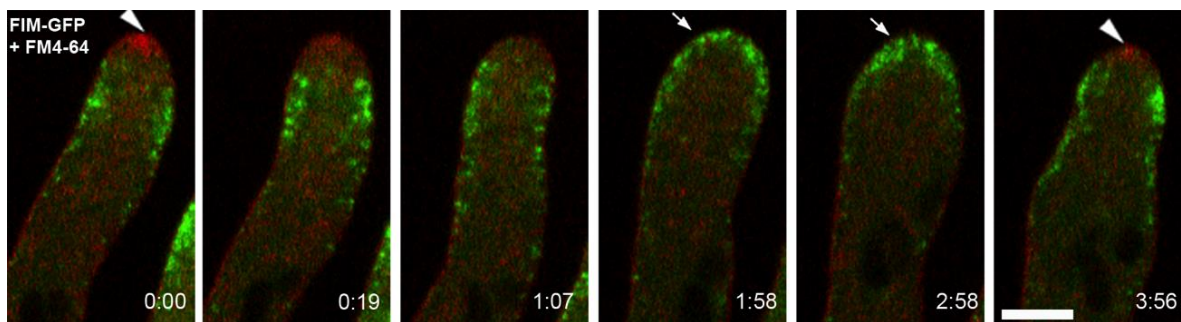
Figure 8: Actin patches delocalize when growth is disrupted. After the disassembly of the Spitzenkörper (arrowhead), actin patches lost their subapical localization and reach the swollen tip (arrowheads). When the Spitzenkörper is reassembled, the patches recover their subapical localization. Scale bar = 5 µm.

To validate the apparent collar shape of the actin patches, as well as the position of actin in the Spitzenkörper, a 3D reconstruction of confocal z-stacks of Lifeact fluorescence was performed. In these reconstructions it is possible to observe that the patches formed a complete collar around the hyphal subapex (Fig 9, Movie 5).
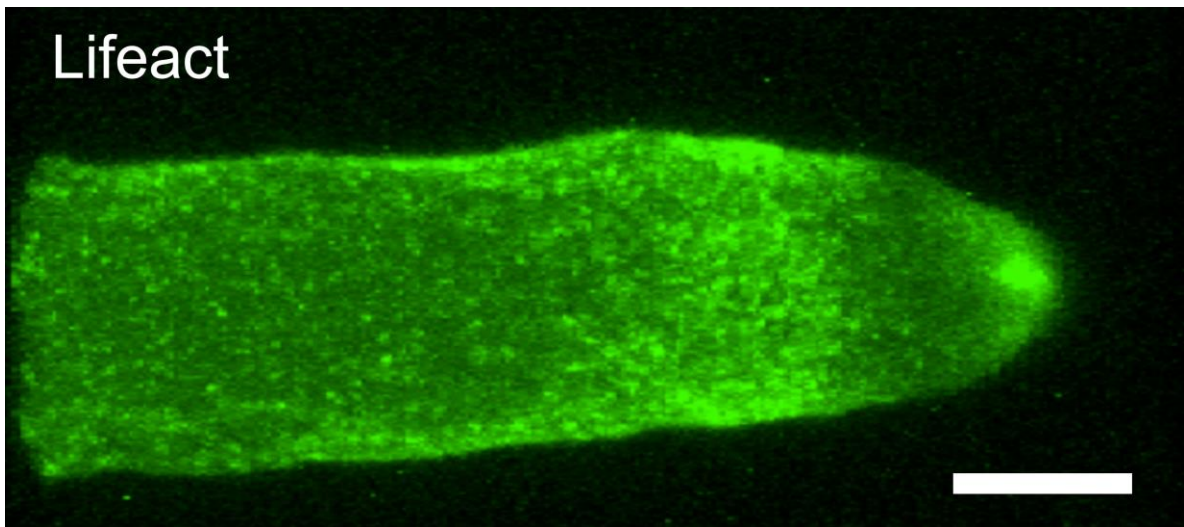
Figure 9: Three dimensional projection of z-stack confocal images of Lifeact. Actin is located in the cellular cortex and also in the Spitzenkörper. Scale bar = 5 μm.

4.2 Actin Patches are Mobile

Total Internal Reflection Fluorescence Microscopy (TIRFM) imaging confirmed that actin patches were located in close proximity to the plasma membrane. The high temporal resolution of TIRFM allowed a thorough analysis of the mobility of F-actin patches labeled with Lifeact, FIM-GFP and ARP-3-GFP (Fig. 10, Movie 6). Patches moved independently from each other; either towards the apex (anterograde motion) or to the distal parts of the hyphae (retrograde motion) (Fig 10. Movie 6). Close to the apical region almost all of the patches (> 90 %; n= 30) moved towards the apex, and in older parts of the mycelium the proportion exhibiting anterograde movements decreased (~ 70 %; n= 30). Actin patches were

classified depending on their mobility in two general types: mobile patches and static patches, although a single patch could exhibit both types of movement. Patches were most often static, and such patches were distributed all throughout the cell. Static patches may suddenly become mobile and a moving patch may stop moving. The speed of the patches labeled with Lifeact was 3.7 ± 0.2 µm s^{-1} and with FIM-GFP it was 3.0 ± 0.1 µm s^{-1}. Most of the patches that comprise the subapical ring are static (Fig. 10 Movie 6). In the basal region, the majority of the patches are mobile with sudden fast movements that alternate with periods of no movement at all. The patches seemed to follow the tracks of cortical F-actin cables (Fig. 10). The time a patch was visible is defined as the patch lifetime. The average lifetime of a patch was 5.2 ± 0.35 s (n=30). Some patches exhibited little or no lateral movement within a given focal plane before their inward movement (Fig. 10), and some were displaced considerably before leaving the focal plane (Fig. 10).
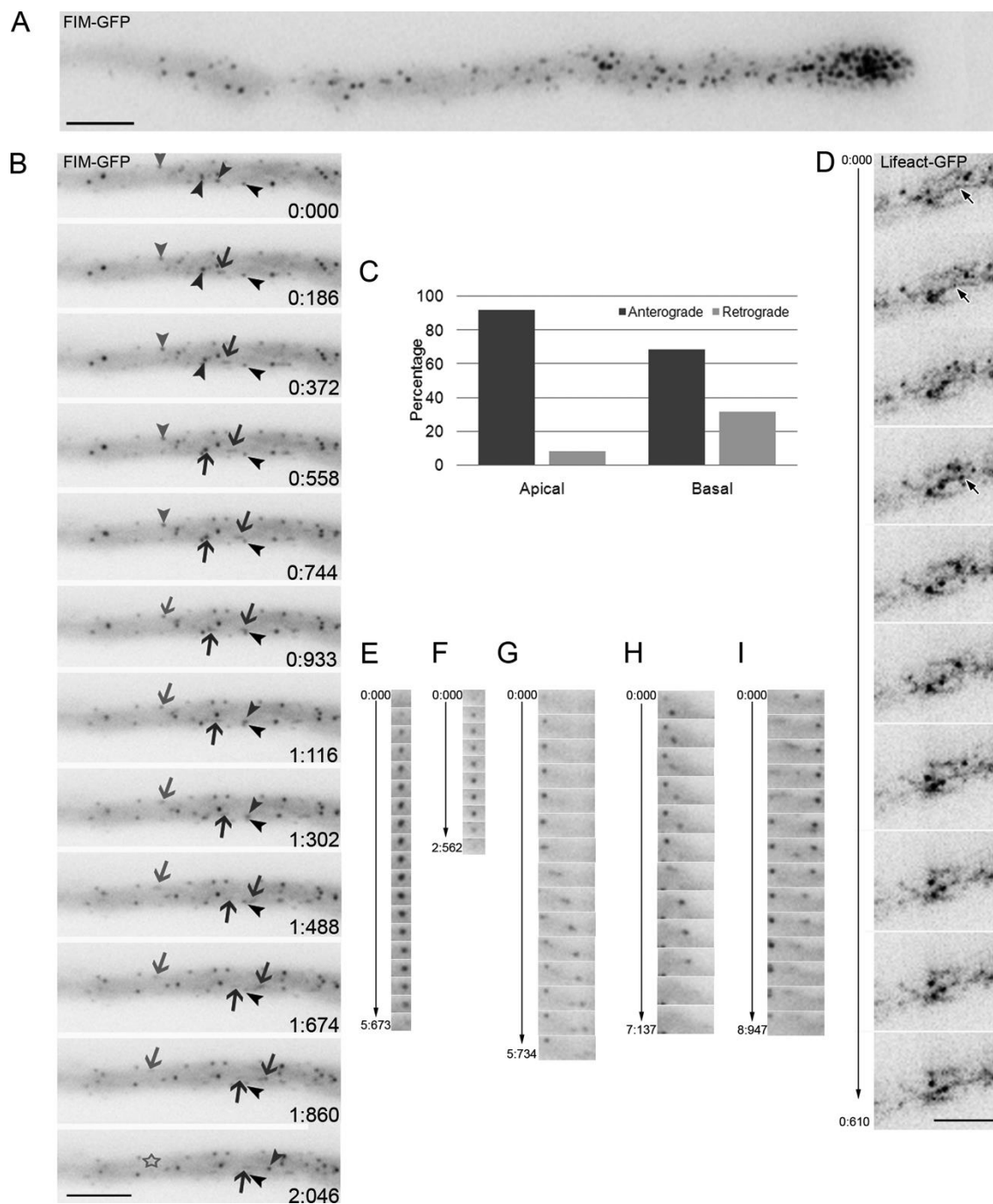
Figure 10: Actin patch dynamics and lifetime. FIM-GFP labeled patches (A-C, E-I) and Lifeact-GFP labeled patches and cables (D). (A) FIM-GFP patches in the apical and subapical region. (B) TIRFM Time series of the subapical region, some instances of patches are pointed to follow their trends. Each patch is pointed by arrowheads and arrows of different grey scale. Arrowheads were used to mark the patches when there was no movement and arrows indicate the movement, the star show a patch that disappeared

from the focal plane. Patches during movement seem elongated structures. (C) Graph of the relative frequency of patches anterograde and retrograde movements in apical and basal regions. (D) Detail of a time series of the subapical region of a strain labeled with Lifeact-GFP. Black arrows show the association between F-actin cables and patches (see Movie 6- it is possible to observe how patches follow the cable track), (E-I) Time series of individual patches lifetime, some patches travel short distances before plasma membrane detachment (G-I) and some stayed in the almost the same place (E-F). Scale bar for A, G and H = 10 μm and for B-F = 2 μm. (I) Time is shown in sec:msec.

4.3 GFP-Immunoelectron Microscopy Of ARP-2-GFP. Endocytic vesicles labeled with ARP-2-GFP immunostaining

The two-step immuno-EM protocol described by Buser and McDonald (2010) for labeling GFP-tagged proteins was implemented for *N. crassa* for the labeling of actin patches. Mature endocytic vesicles are coated with actin nucleated by the Arp2/3 complex. The preservation of the hypha with the fixation technique was sufficient to maintain the cellular integrity. The structure of the hypha was well conserved; internal cellular features were well maintained, as indicated by the homogeneity of the cytoplasm, the shape and integrity of mitochondria and the presence of actin microfilaments and microtubules (Fig. 11).

Rounded structures with an average diameter of 82.01 nm (n = 30; SD = 9.71) were seen closely associated to gold nanoparticles, indicating positive labeling of ARP-2-GFP (Fig. 11). The surface area was calculated using the formula $A=4\pi \cdot r^2$. The average surface area of these vesicles was 21, 427.28 nm^2 (n = 30; SD = 5,137.71). These structures were therefore considered putative endocytic vesicles. The sectioning plane was not completely parallel to the hypha; therefore oblique sections were collected. As expected, nanoparticles were more

abundant closer to the vicinity of the subapical region than distal regions of the cell. In the negative controls, treated with secondary but not primary antibodies, no labeling was detected. Gold nanoparticles were not present when ARP2-2GFP sections were treated only with primary antibody but not with secondary antibody (Fig. 12).
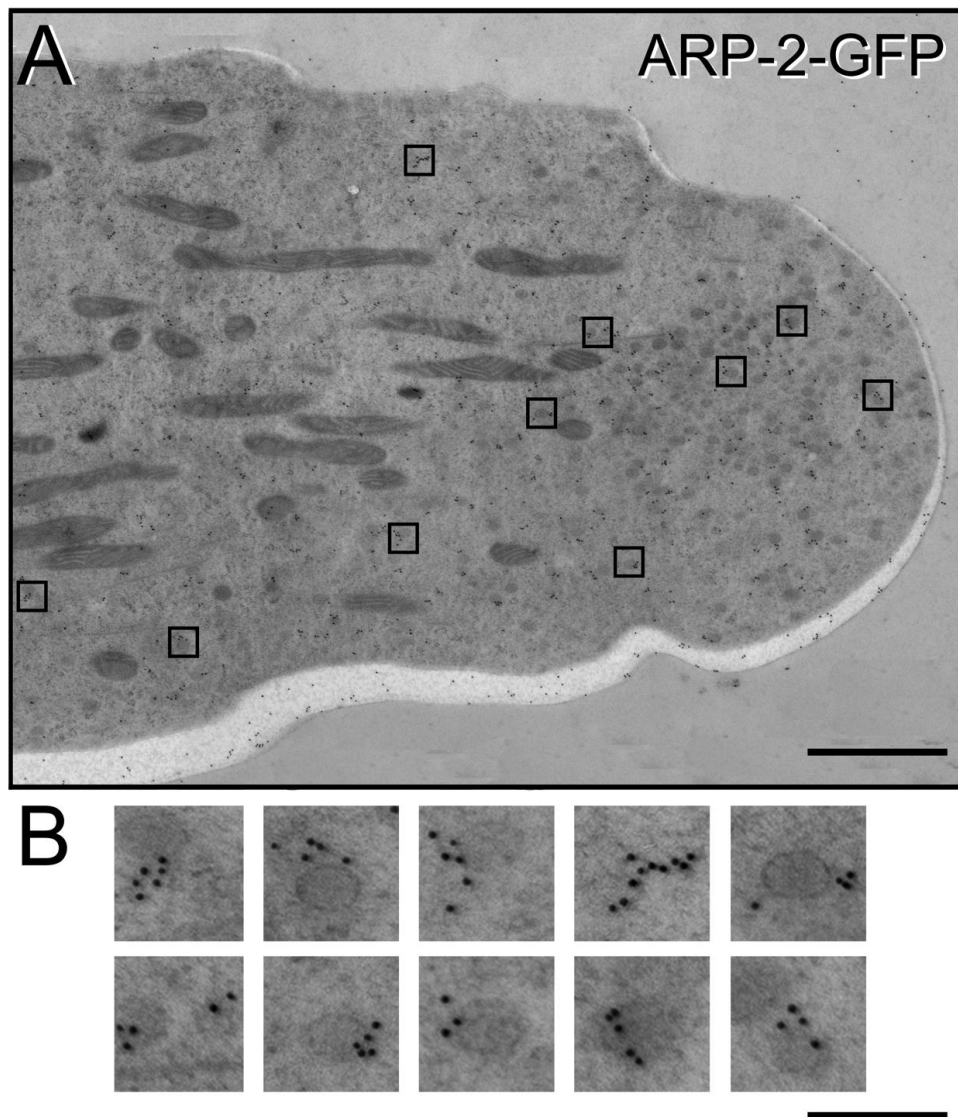
Figure 11: GFP-Immunoelectron micrograph. A) Cortical section of a hyphal tip of the *N. crassa* strain expressing ARP-2-GFP treated with primary

antibodies anti-GFP (rabbit), and secondary antibodies anti-rabbit FC coupled to 10nm gold nanoparticles. Scale bar = 1 µm. B) Vesicles (outlined in A) displaying a clear GFP-immunolabeling. Scale bar = 250 nm.
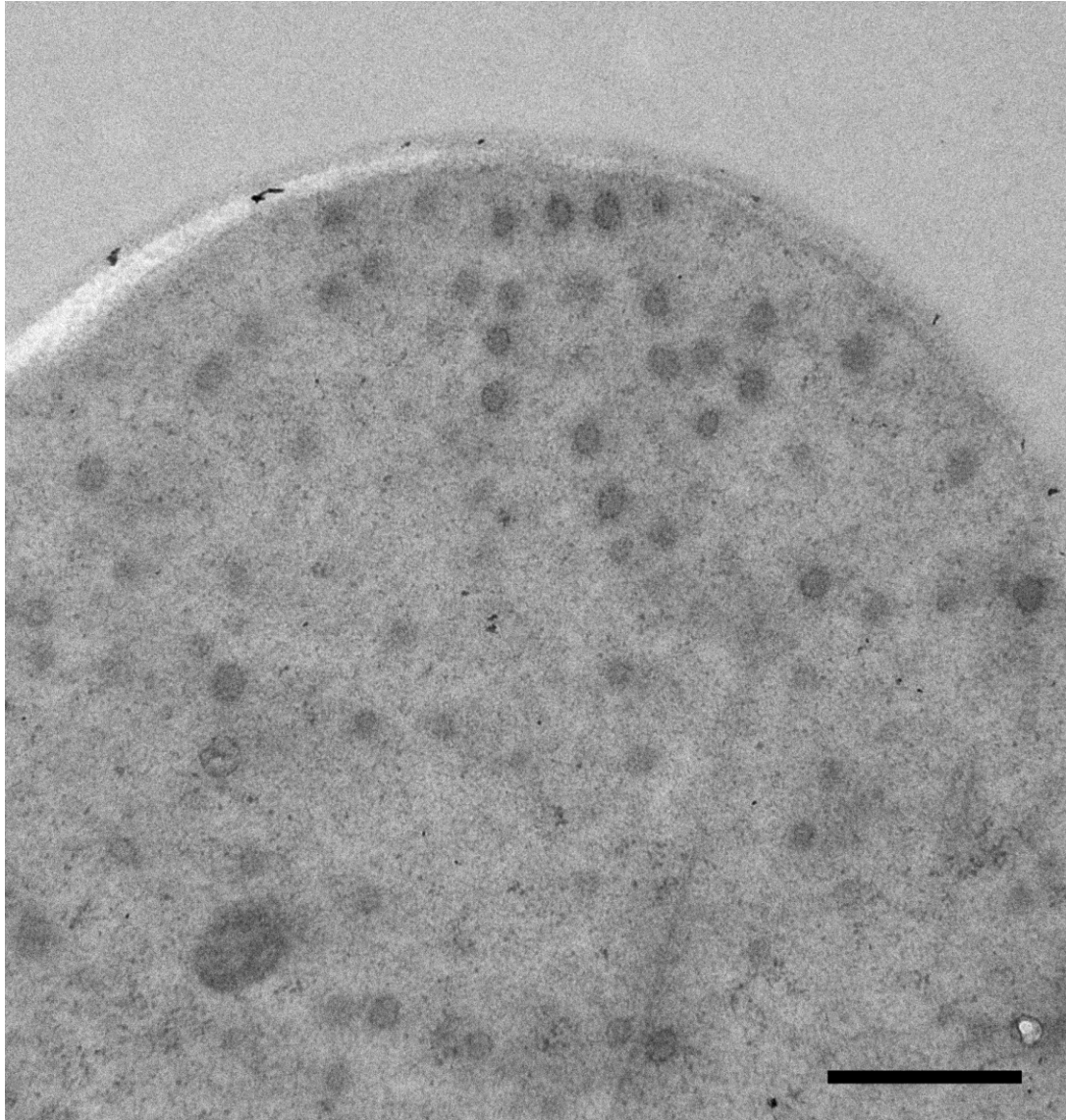
Figure 12: GFP-immunolabeling negative control. Gold nanoparticles were not present in this section of an ARP2-2GFP strain treated only with primary antibody but not with secondary antibody. Scale bar =500 nm

Table 2: Endocytic vesicle dimensions. Average (AVG), Standard Deviation (SD)

(n=30)	Diameter (nm)	Area (nm^2)
AVG	82.01	21,427.28
SD	9.71	5,137.71
AVG-SD	72.29	16,289.58
AVG+SD	91.72	26,564.99

4.4 Depolymerization Of The F-Actin And Microtubular Cytoskeleton

In order to confirm the usefulness of the actin cytoskeleton reporters, disruption assays were performed in the strains expressing Abd2-GFP, ARP-2-GFP, Lifeact and TPM-1-GFP. All strains showed a disruption of the fluorescent pattern when exposed to the F-actin depolymerizing drugs cytochalasin A (Cyt A) and latrunculin A (Lat A) (Fig. 13). To address the distribution of F-actin structures in cells treated with anti-actin drugs, we observed two focal planes: the plane closer to the plasma membrane (Fig. 13A) and the middle plane (Fig. 13B). In Abd2-GFP and ARP-3-GFP, the subapical ring had disappeared and all the patches where scattered and reached the apical dome in both Cyt A and Lat A treatments (Fig. 13A and B). Patch movement was severely diminished, although the patches did not disassemble (Fig. 13A and B). In the strains tagged with TPM-1-GFP and Lifeact-GFP, neither cables nor the apical accumulation appeared. In the Lifeact strains only patches were visible after treatment (Fig. 13 A and B).

Additionally, the different strains were exposed to benomyl, a microtubule-depolymerizing drug. The motility of Abd2-GFP patches was not affected, but they

were delocalized. The apical ring was not present and many patches accumulated in the apex (Fig.13 A and B), thin cables labeled with TPM-1-GFP and Lifeact were present in cells treated with benomyl (Fig. 13A and B), Lifeact patches were spread in the apex and subapex (Fig. 13A and B). Taken together, these results indicate that the ABP reporters faithfully present actin motility in living cells, and that microtubule-depolymerizing drugs only marginally disturb their movement.
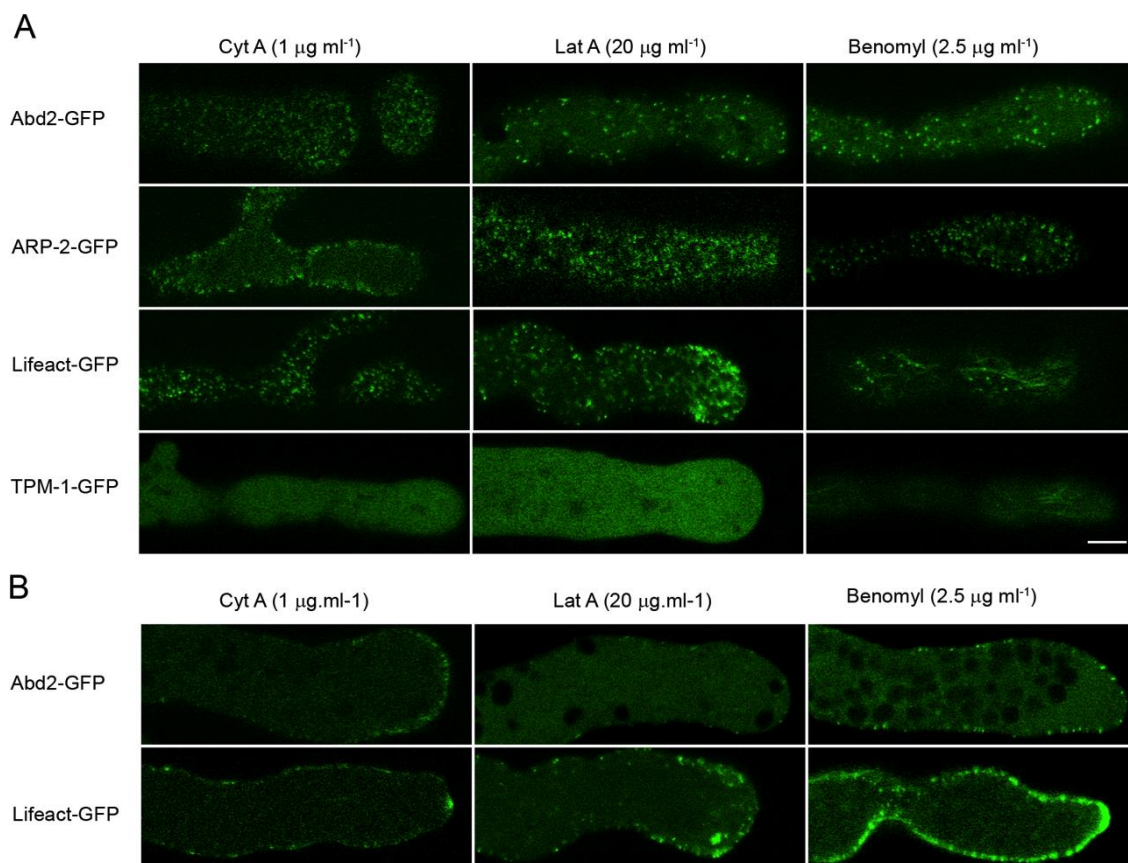
Figure 13: Confocal images of cells treated with actin inhibitors Cyt A and Lat A and microtubule inhibitor benomyl. Two different focal planes are shown, (A) Plane closer to the plasma membrane and (B) Central plane. Scale bar = 5 μm.

4.5 Organization of the actin cytoskeleton during morphogenetic events

4.5.1 Actin accumulates at branching sites

At the onset of branch formation cortical Abd2-GFP and ARP-3-GFP patches subtending the branching site became associated laterally with the incipient branch. As the protruding branch emerged, these patches followed the contour of the developing branch (Fig. 14). Upon continued branch elongation, the continuity of the patches was broken and they resolved into two collars, one associated with each growth site and maintaining a constant distance from the associated apex (Fig. 14). TPM-1-GFP appeared just before it was possible to observe the emergence of the branch (Fig. 15 Movie 7) and TPM-1-GFP fluorescence was localized in the apex of the branch all the time.
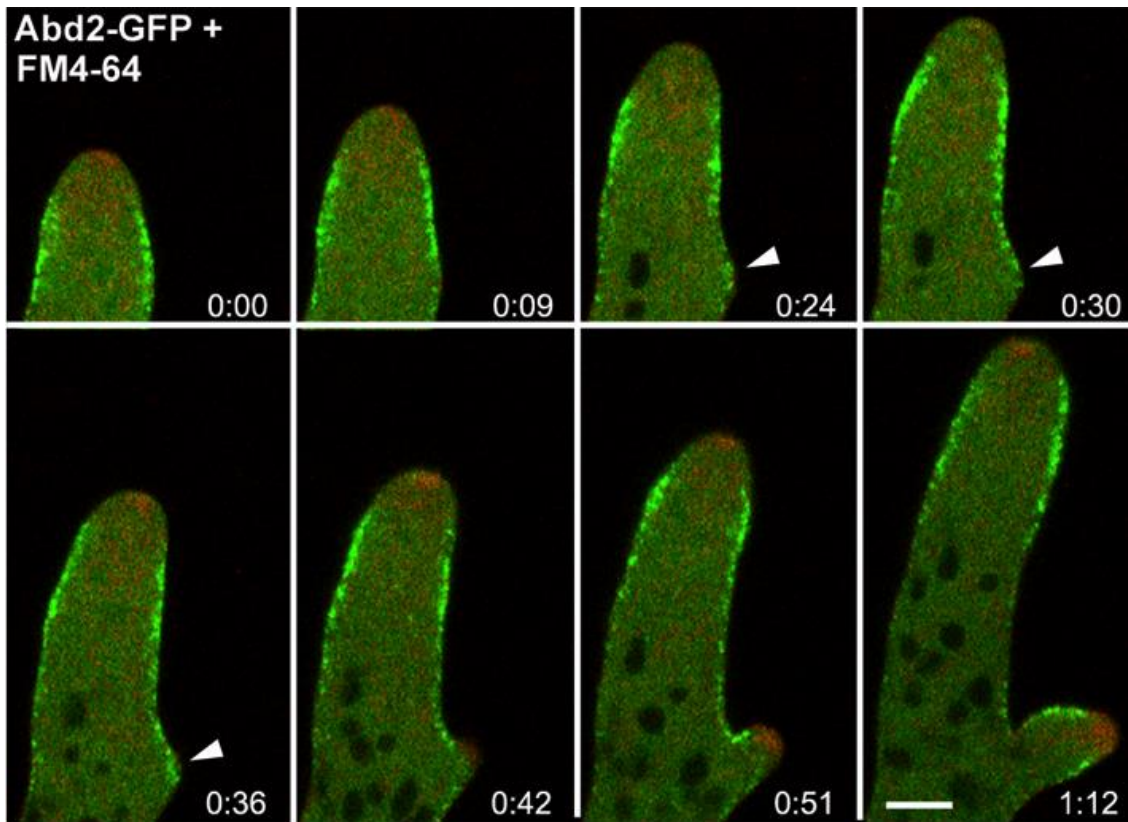
Figure 14: Actin patches assemble at branching sites. Distribution of actin patches is relocated to sites of active growth i.e. a branching site. Arrowheads point to actin patches at a developing lateral branch. Scale bar = 5 µm.
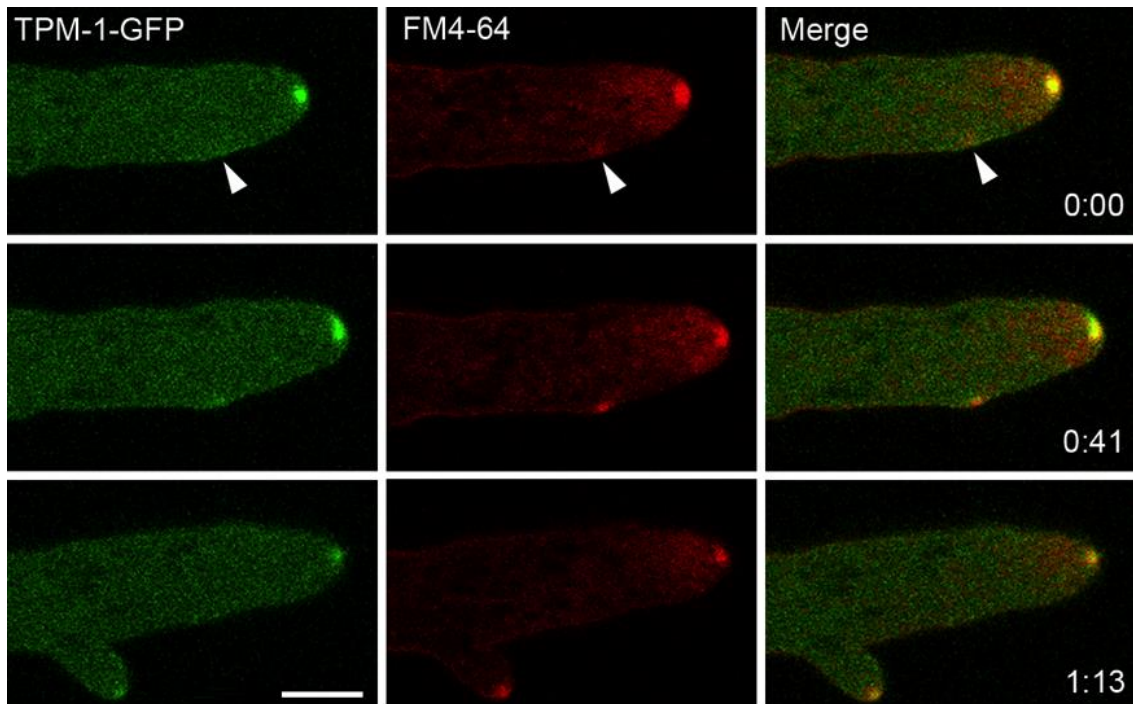
Figure 15: A new Spitzenkörper is assembled at branching sites. Arrowheads indicate to an incipient lateral branch. The branch Spitzenkörper is associated with Tropomyosin. Scale bar = 5μm.

4.5.2 Actin accumulates at septation sites

4.5.2.1 Septal Actomyosin Tangle formation: the initial step in septation

Septum formation is a complex process that proceeds through a series of events, of which the first one is the selection of the septation site, followed by the assembly of a contractile actin ring and culminating with the joint action of plasma membrane ingrowth and cell wall deposition. Each event is related to a particular subset of proteins that are tightly regulated. In order to compare the timing of

appearance of key proteins, an arbitrary time zero was defined as the moment at which plasma membrane starts to grow (Fig. 16).
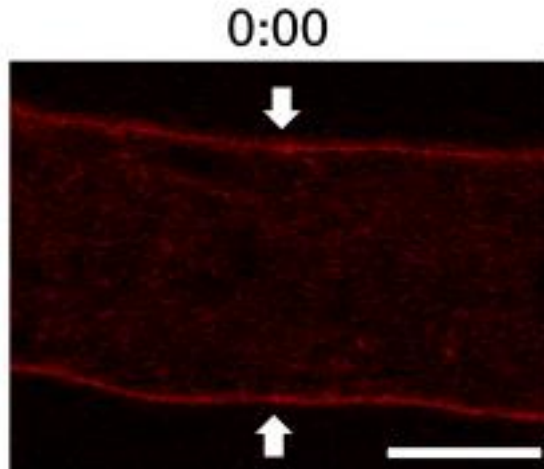
Figure 16: Defining Time zero. Time zero (0:00) is the moment at which membrane ingrowth is detected. Arrows point to incipient ingrowth of plasma membrane in a future septation site. Scale bar = 5 μm.

Growth of the septum starts with the formation of an actomyosin web-like pattern following the contour of the hypha. This structure, named the Septal Actomyosin Tangle (SAT), is a conspicuous tangle of actin filaments associated with tropomyosin and class II myosin (MYO-2). The SAT then assembles into a Contractile Actomyosin Ring (CAR). The first indication of SAT formation was short actin cables in the cell cortex 6:20 min:sec before plasma membrane ingrowth (0:00 min:sec) in the region where a new septum would form (Fig. 17).
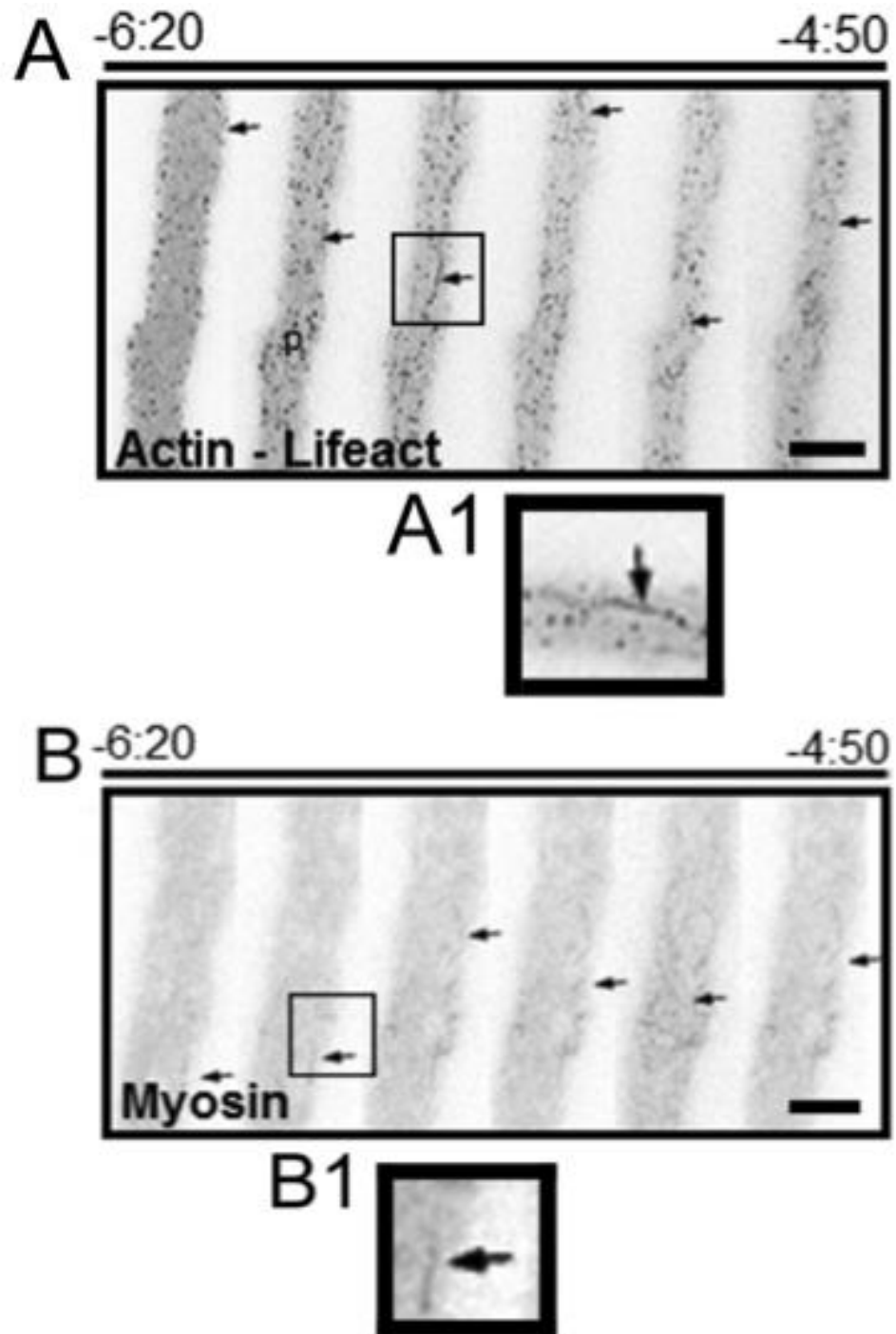
Figure 17: Actomyosin cables are the earliest components to localize at future septation sites. Panels (A) and (B) show formation of actin and MYO-2-GFP short filaments prior to septum formation. Selected regions A1 and B1 (squares in A and B, respectively) show short cables. Scale bar = 5µm.

Cortical actin cables extended exhibiting a marked helical tendency and a longitudinal orientation parallel to the hyphal axis. The filaments increased in number and thickness progressively forming a cortical meshwork of actomyosin cables. The SAT covered an average length of 35 µm and its formation took place at about 165 µm from the apex (n=17). The SAT was completely formed at -4:30 ± 0:30 min:sec (n=18) (Fig. 18). As is true for other actin cables, the localization of the SAT cables was the cell cortex, as demonstrated by a three dimensional reconstruction (Fig. 19, Movie 8). Tropomyosin (TPM-1-GFP) appearance coincided with the presence of the SAT (Fig. 20) as part of the actomyosin tangle.
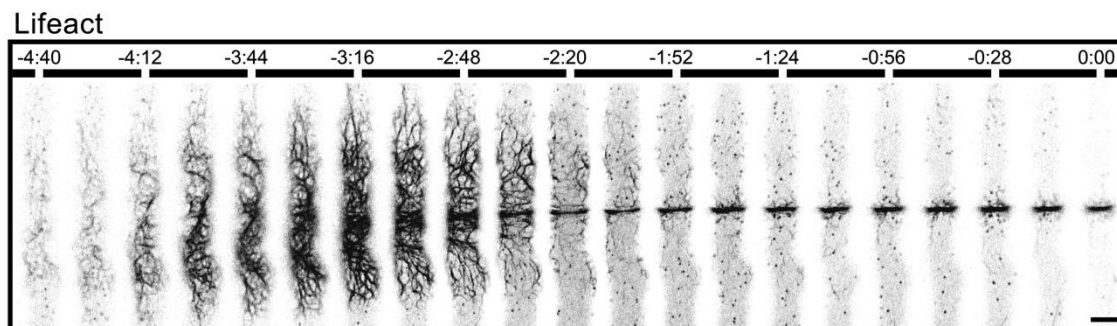
Figure 18: Dynamics of Septal Actomyosin Tangle (SAT) formation and its transition to CAR. Each panel is a series of confocal images taken at 15 sec intervals showing the assembly of the SAT and the conversion of SAT to a constriction ring (CAR). Lifeact was imaged near the hyphal cell. Time 0:00 signals the earliest moment of membrane invagination. SAT assembly reached a peak at -3:00. Note actin patches (p) are absent during the SAT stage and begin to appear after CAR formation from time -4:40 to -2:20 the helicoidal actin cables coalesce to from a proto CAR that is finally assembled into a CAR at approximately -2:30 (see Movie 8). Scale Bar = 5 µm.
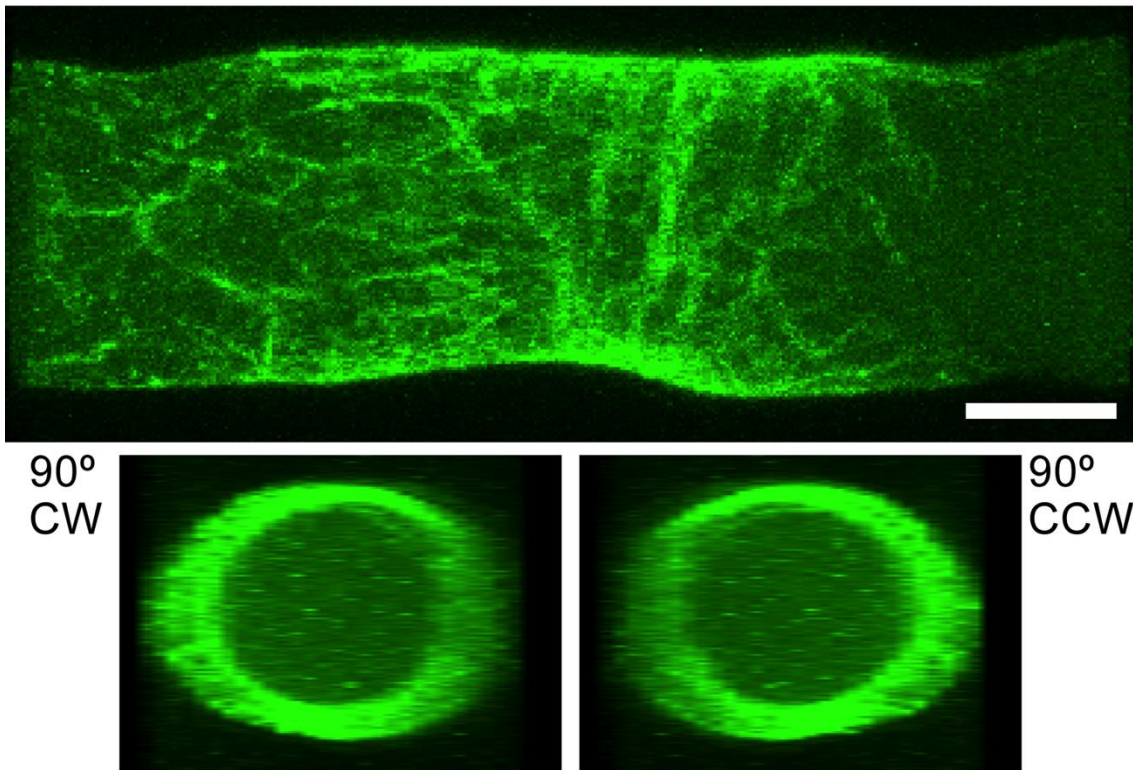
Figure 19: The Septal Actomyosin Tangle is composed of helicoidally arranged cables in the cellular cortex. Longitudinal and transverse views of the rotated construct show the tangle of roughly helicoid actin cables in the cell cortex. Scale bar = 5µm.
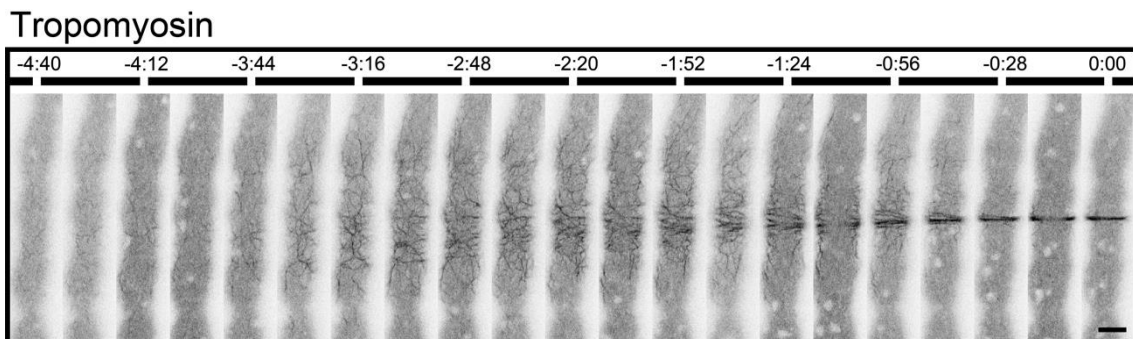
Figure 20: Assembly of the Septal Actomyosin Tangle labeled by tropomyosin (TPM-1-GFP). Tropomyosin forms the same pattern as the one imaged by Lifeact fluorescence. Scale bar = 5 µm.

4.5.2.2 Transition from SAT To CAR

The SAT reached its maximum expression in both number and thickness of filaments at about -3:00 min (Fig. 18). The collection of helicoidally extended cables began to compress longitudinally towards a mid-point in the tangle. Compaction of the SAT was not symmetrical; the anterior side of the tangle seemed to contribute more cables to the CAR than the posterior side. The first evidence of a ring appeared at about -2:48 min:sec. This structure is referred to as the proto-CAR to emphasize that this ring had not reached its final place or size. Actin cables continued to condense while the proto-CAR migrated forward a distance of ~4 μm until it became the final CAR (Fig. 21). The CAR was assembled at -2:00 min, but its constriction started at zero time (Figs. 18 and 21). The complete process of SAT and CAR formation is a spectacular event that lasted ~10 minutes (n=18); it can be seen in abbreviated fashion in Movie 9 (Fig. 18). The next phase, from plasma membrane ingrowth to septum completion, took approximately 5:30 min.

-3:00

CAR
assembly

-2:00
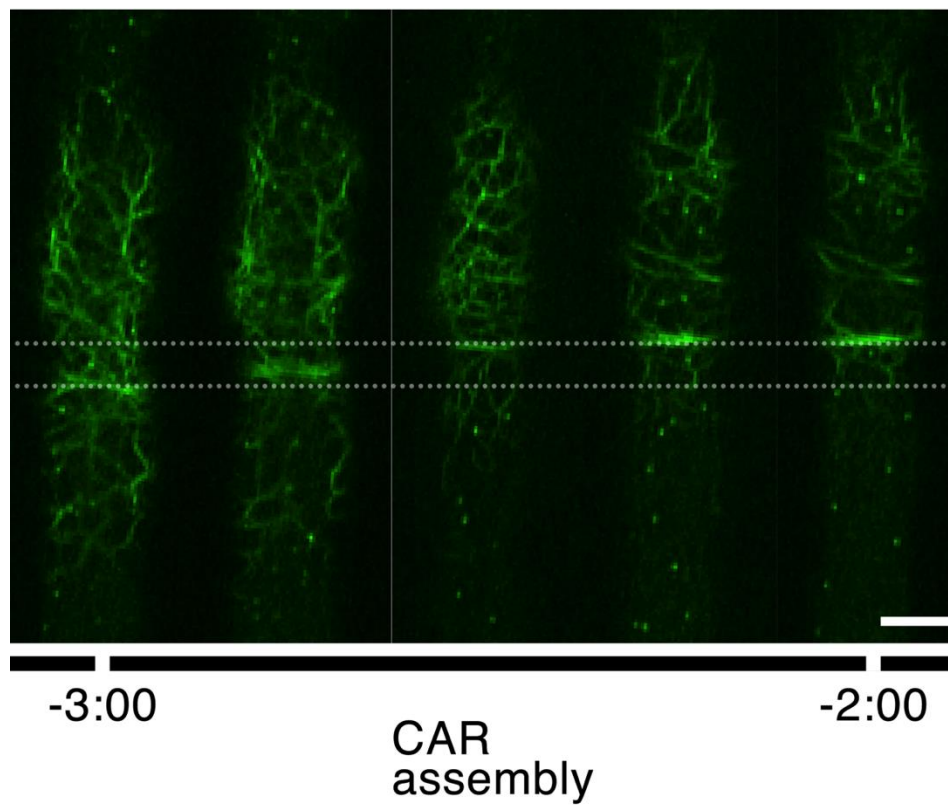
Figure 21: Details of the assembly of proto-CAR and its maturation into a CAR. Dotted lines frame the zone of displacement of the ring (4 µm for this particular hypha). Scale Bar = 5 µm.

4.5.2.3 Wave of polymerization

SAT formation was a discrete event in a wave of actin polymerization, a tenuous cloud of Lifeact fluorescence that traveled toward the tip from one septation site to the next (Fig. 22).

The pulse of fluorescence advanced from the proximal edge of the current SAT to the next septation site at a speed of 0.4 $\mu m \cdot s^{-1}$, twice the hyphal growth rate (Movie 10). Within the cloud of fluorescence it was possible to visualize some small actin cables that traveled from the SAT currently in formation to the next septation site (Fig. 22 A). A surprising event was the occasional abortion of the CAR formation process. A SAT began to assemble in the expected site but never fully developed, after it started to coalesce to form the ring, it became dispersed and no septum was formed. Instead, some of the remaining cables reassembled at some distance to give rise to a normal septum (Fig. 22 B).
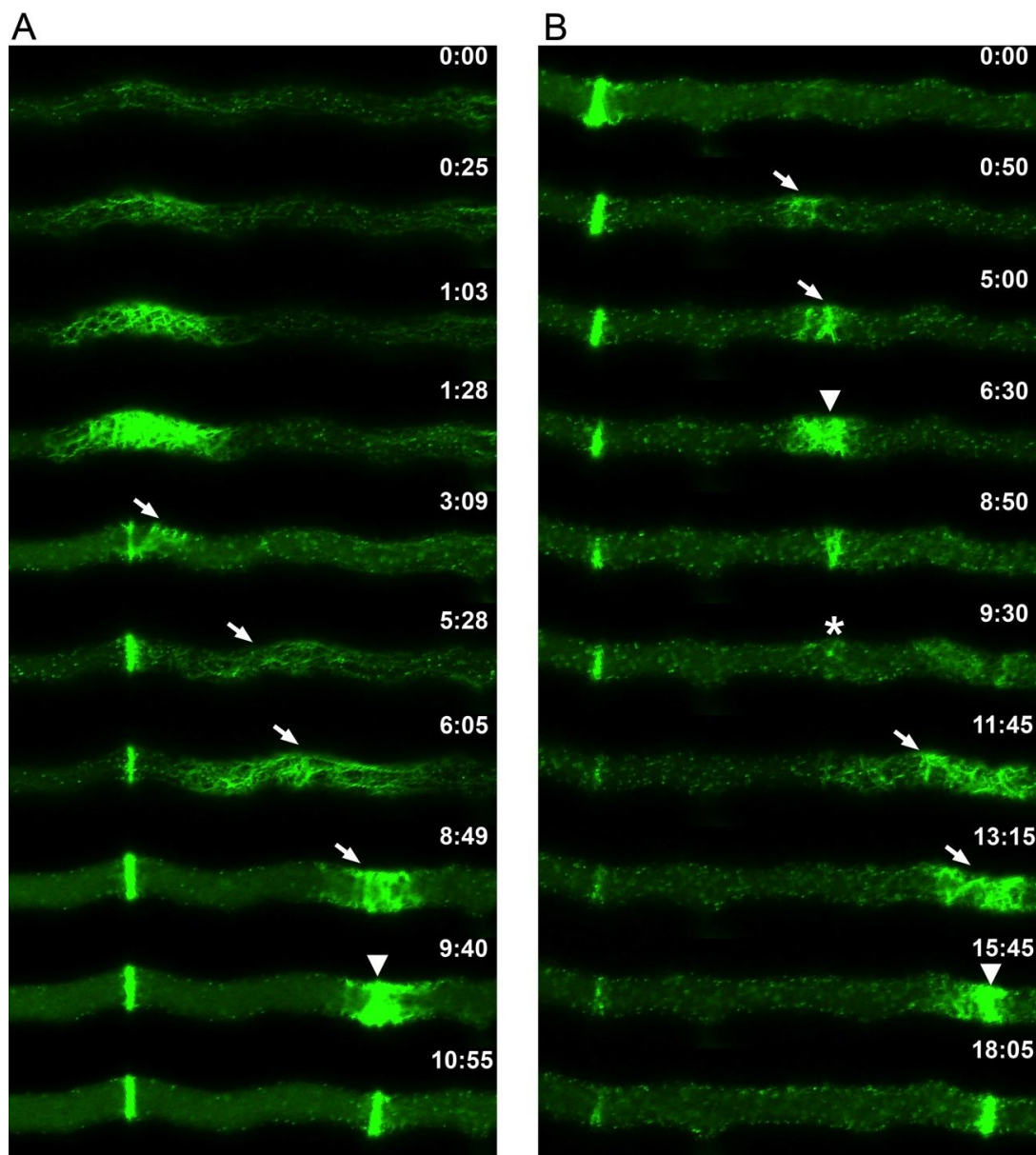
Figure 22: Details of SAT and CAR assembly during septation. An instance of CAR abortion. (A) Normal septation. Actin cables emanate from a recently formed septum and assemble a new SAT that moves towards (arrows) the next septation site where it coalesces to form a CAR (arrowhead) (B) CAR abortion. In this instance, a SAT began to be established at the expected site (arrowhead); by 6:30 it had reached a maximum size which was much smaller than a normal SAT and by 9:30 it had almost disappeared (asterisk); no septum was formed, instead the actin cables from the remains of the aborted CAR migrated towards a new site (arrows). This time the SAT proceeded to form a normal CAR (arrowhead). Scale Bar = 10 μm.

4.5.2.4 Recruitment of Actin-Binding Proteins during CAR formation

The constricting actomyosin ring is a complex structure made of actin filaments anchoring other proteins related to actin function (myosin, formin, and tropomyosin) that make it a functional constricting ring. F-Actin in the developing septum exists in two configurations: contractile cables and patches.

In the innermost region of the actin ring, tropomyosin co-localized with actin, as revealed by a tetradimensional reconstruction of a Lifeact/TPM-1-mChFP fusion. TPM-1-ChFP did not colocalize with actin patches (Fig. 23).

Lifeact-GFP
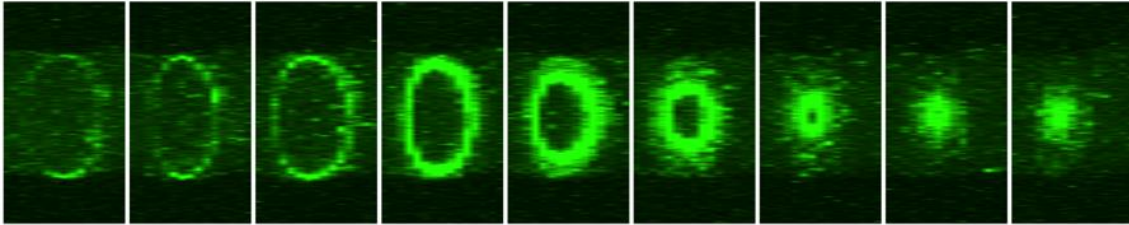
TPM-1-Cherry
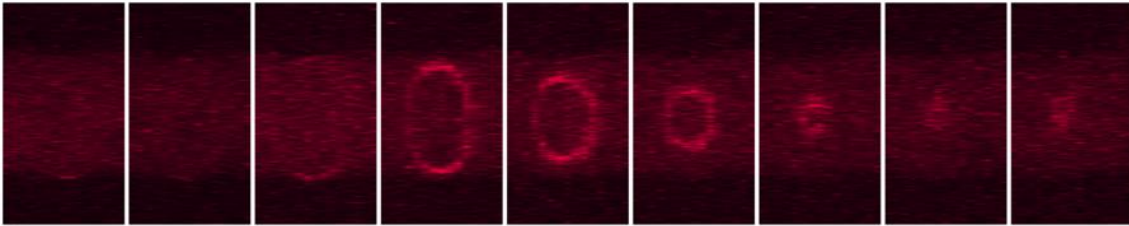
Merge
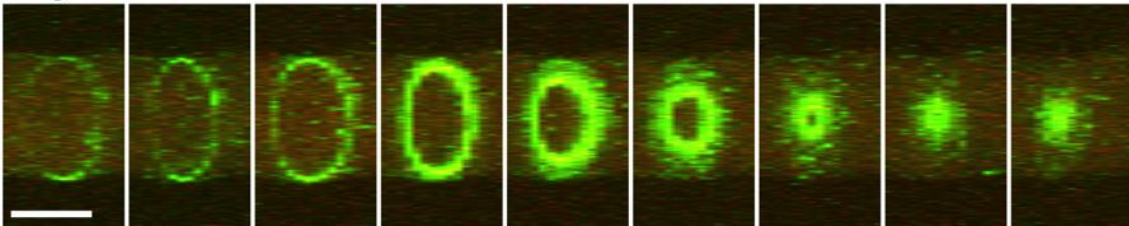
Figure 23: Tropomyosin co-localizes with actin in the Contractile Actomyosin Ring (CAR) during septum growth. Tetradimensional reconstruction of a developing septum in a cell co-expressing Lifeact and TPM-1-ChFP. Scale bar = 5µm.

Scattered patches of Abd2-GFP, FIM-FGP and ARP-3-GFP accumulated around the hyphal perimeter at the septation initiation site (-0:13 ± 0:10 min:sec). Actin patches formed double ring flanking the ingrowing plasma membrane. These rings did not co-localize with the CAR (Fig. 24, Movie 11). An orthogonal view exposed that as the plasma membrane contracted, the patches also moved inward (Fig. 24). When the septum was completed, the fluorescent patches disappeared from both faces (8:31 ± 2:49 min:s).
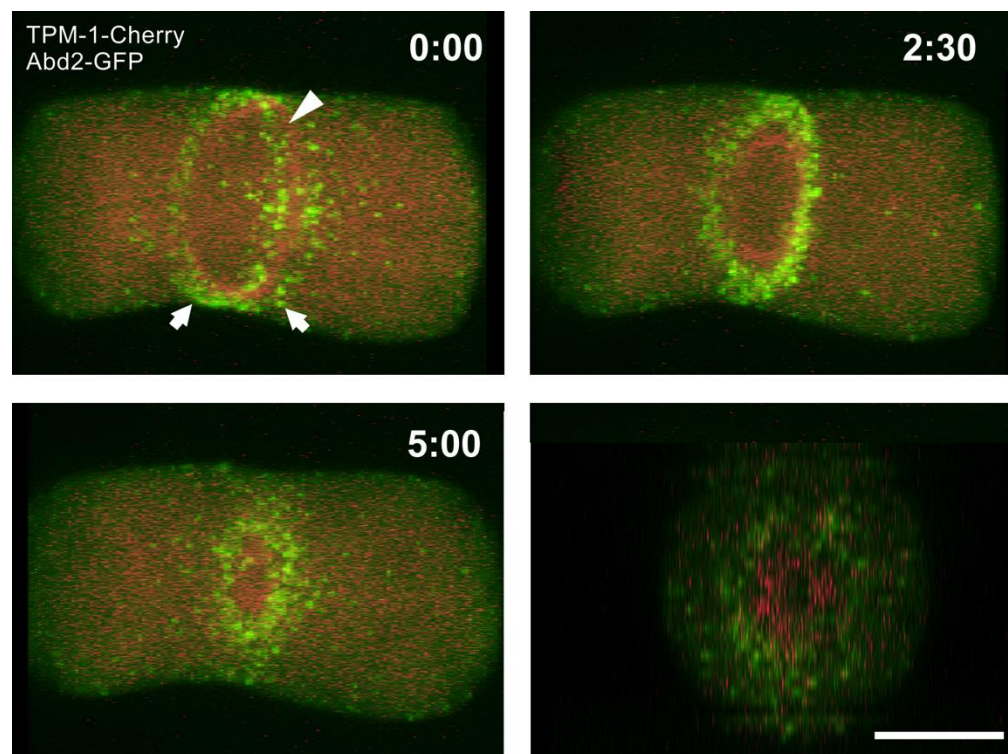
Figure 18: 4D reconstruction of a developing septum in a cell co-expressing Abd2-GFP and TPM-1-ChFP Actin patches form a double ring flanking the Contractile Actomyosin Ring (CAR). White arrows point actin patches flanking the CAR; the arrowhead points the CAR labeled by TPM-1-ChFP. Scale bar = 5 μm.

4.5.2.5 Recruitment Of Other Proteins To Septum Formation Sites

Actin cables were present during septum formation from its establishment until completion. Other essential proteins, *e.g.* Formin (BNI-1), a putative landmark protein (BUD-4) and a cell-wall synthetizing enzyme (CHS-1) were recruited to the septation site after the actomyosin complex. To find out the order of assembly and the precise location of the proteins involved in septation, the time series in Figs. 25-30 were constructed.

Fimbrin (FIM-GFP) was used as a reporter for the actin patches involved in endocytosis (Delgado-Alvarez *et al.*, 2010); accumulation of actin patches was observed around the septation site ~10 seconds before membrane ingrowth. This accumulation of patches followed the progression of CAR constriction, covering the entire septal plate on both sides producing a double ring-like structure (Fig. 25).

The tagging of actin with Lifeact showed the CAR being established 2:00 min before there was the first evidence of constriction (time 0:00) (Fig. 26). Formin (BNI-1-GFP) appeared as a cylindrical band of ~10 µm in width at -3:20 in the septation site (Fig. 28). This band gradually coalesced into a sharp ring that reached its final width a few seconds before membrane ingrowth. The formin ring followed the advancing edge of the ingrowing membrane and was excluded from the rest of the septum plate. At the end of septation, the formin ring comprised the innermost 1/3 of the septum plate and then disappeared (Fig. 28).
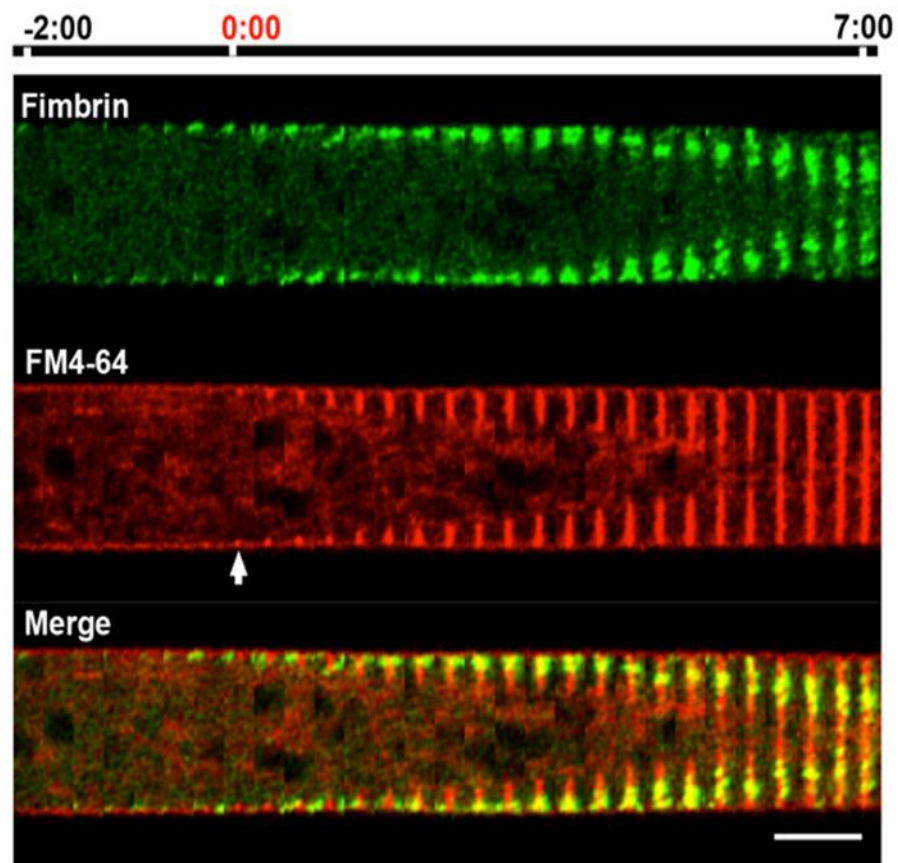
Figure 195: Chronology of Fimbrin in septum development. Series constructed from images taken at 20 sec intervals and assembled to emulate kymographs. Time 0:00 (arrows) signals the earliest moment of membrane invagination. Scale bar = 5 µm.
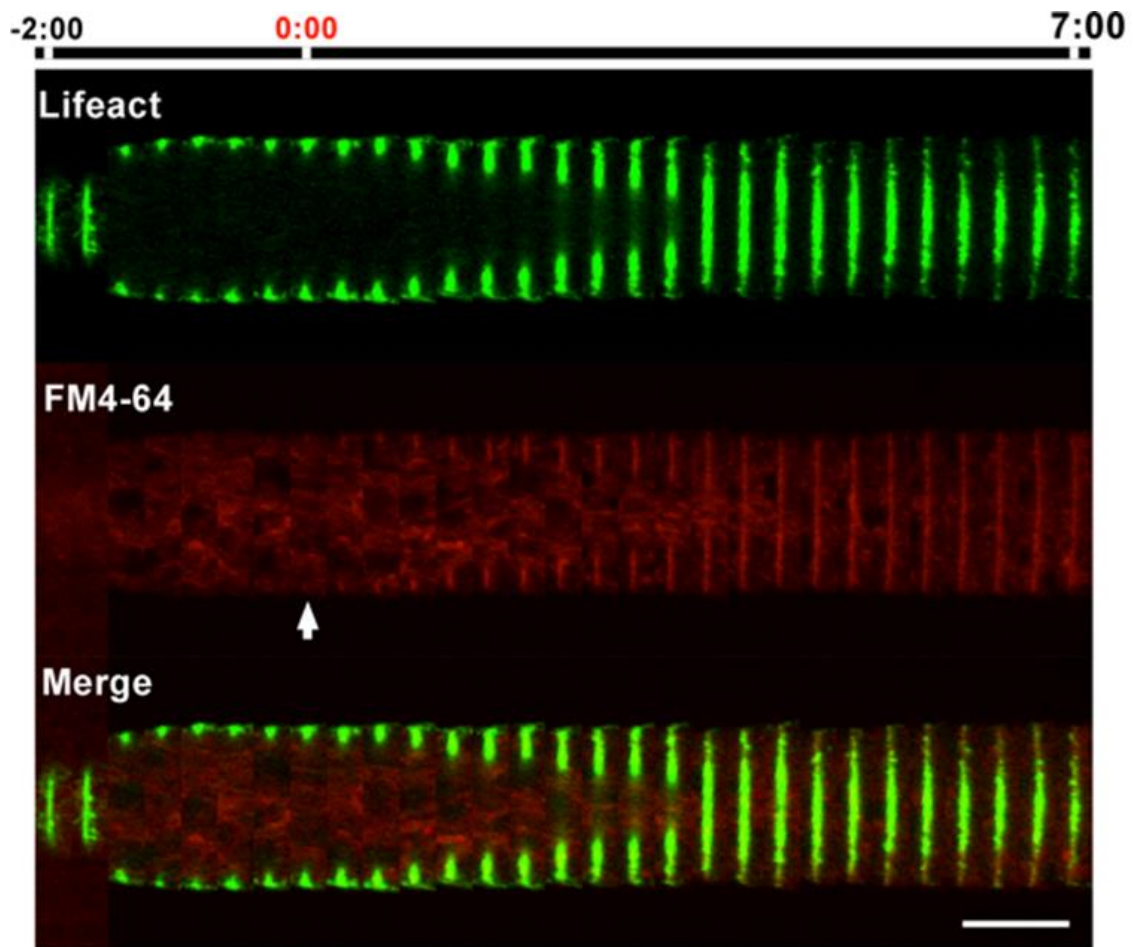
Figure 26: Chronology of Actin (Lifeact-GFP) in septum development. Series constructed from images taken at 20 sec intervals and assembled to emulate kymographs. Time 0:00 (arrows) signals the earliest moment of membrane invagination. Scale bar = 5 μm.
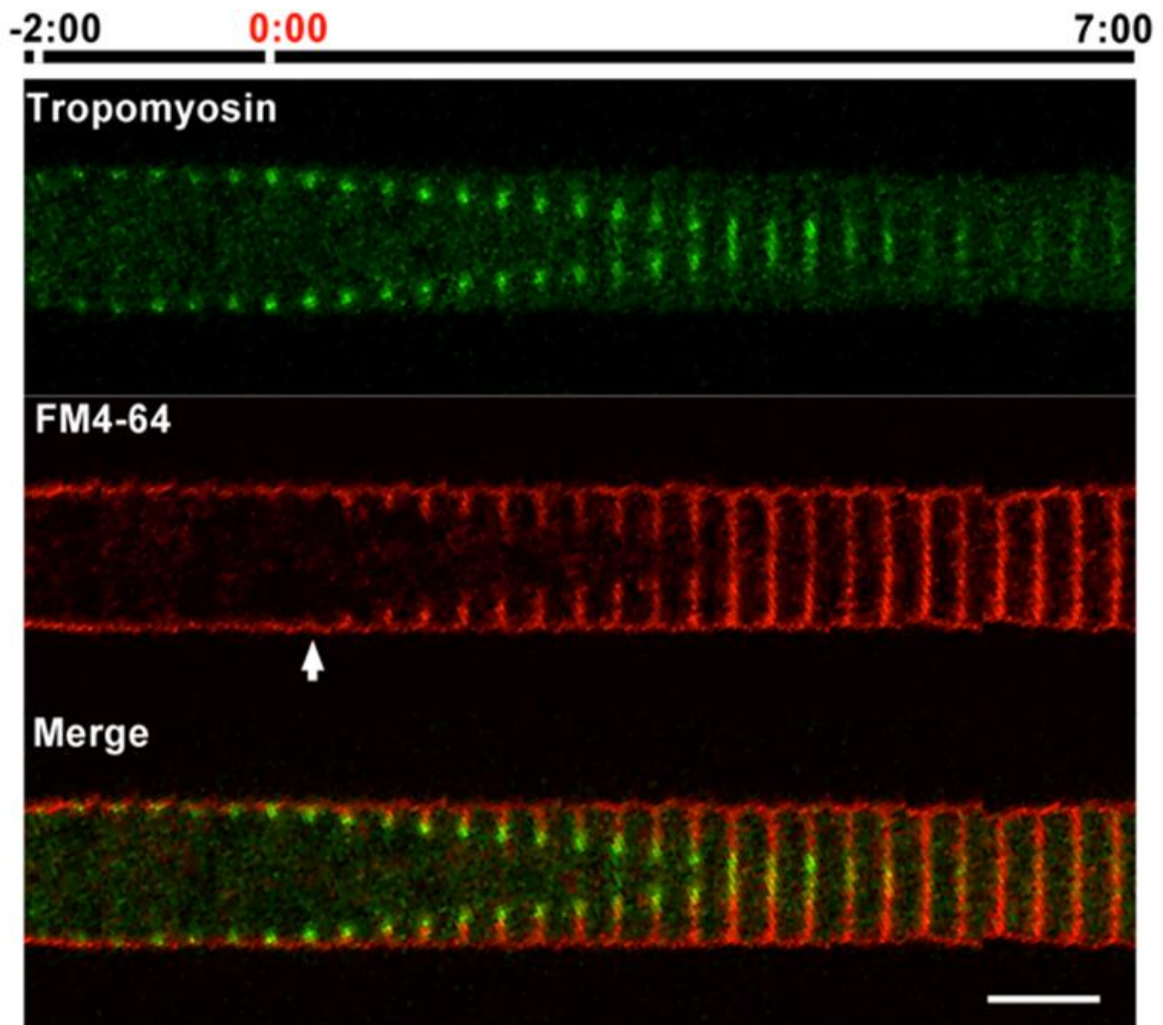
Figure 20: Chronology of Tropomyosin in septum development. Series constructed from images taken at 20 sec intervals and assembled to emulate kymographs. Time 0:00 (arrows) signals the earliest moment of membrane invagination. Scale bar = 5 μm.
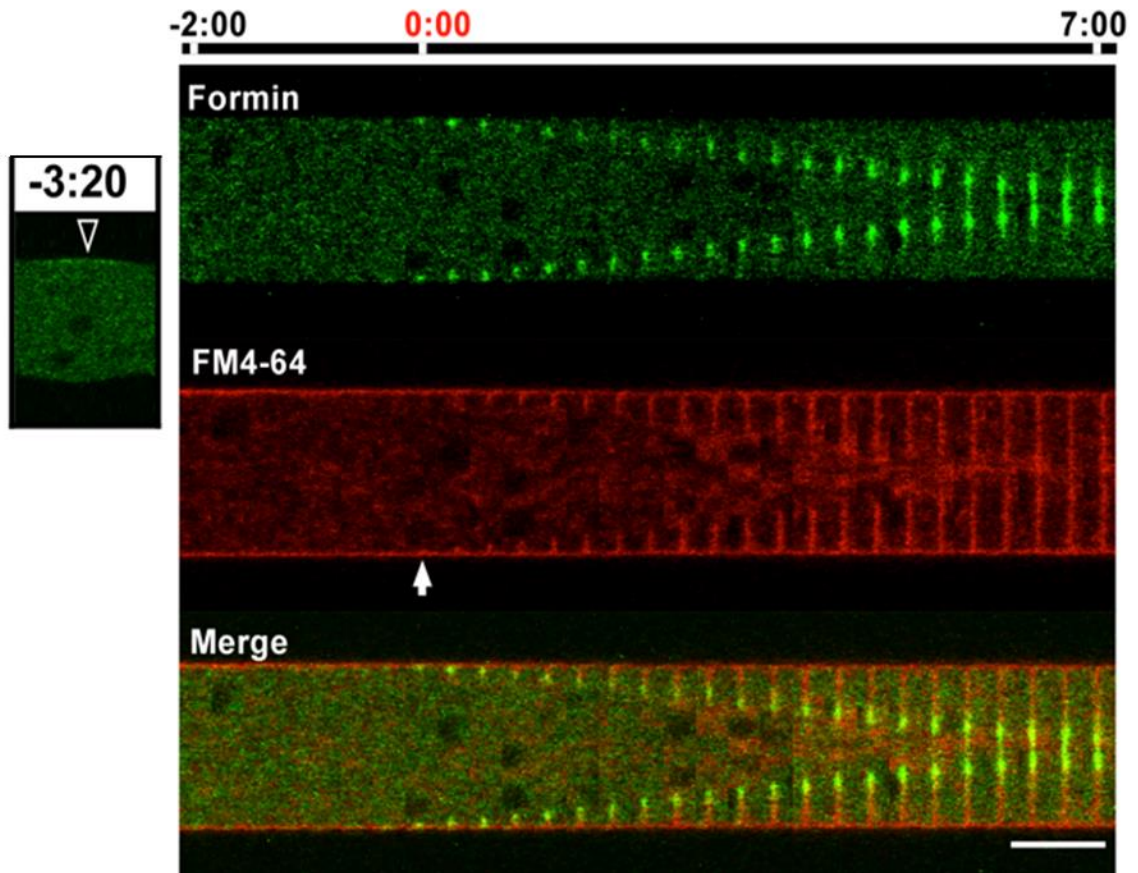
Figure 28: Chronology of Formin in septum development. Series constructed from images taken at 20 sec intervals and assembled to emulate kymographs. Time 0:00 (arrows) signals the earliest moment of membrane invagination. Arrowhead shows the appearance of Formin at -3:20. Scale bar = 5 μm.

BUD-4 is an anillin-like protein that serves as a reporter of the BUD-4/BUD-3/RHO-4 complex (Justa-Schuch *et al.*, 2010). BUD-4-GFP formed cortical spots in the vicinity of the future septation site 2 min before constriction of the CAR. A BUD-4 ring was formed at the leading edge of the ingrowing membrane. At the end of the septation process, BUD-4 covered the inner half of the septum and unlike other markers it remained for the entire observation period (Fig. 29).

The genome of *N. crassa* encodes seven chitin synthases and all of them are present in the septa (Riquelme *et al.*, 2007; Riquelme and Bartnicki-García, 2008; Sanchez-Leon; 2011; Mouriño-Pérez and Riquelme 2013). We found that chitin synthase 1 (CHS-1) began to accumulate ~2:18 min before membrane ingrowth could be detected. CHS-1-GFP fluorescence waned from the cell surface prior to membrane ingrowth. Once membrane ingrowth started, chitin synthase accumulated in the growing edge of the developing septum in synchrony with its centripetal growth (Fig. 30). The timeline of protein recruitment to future septation sites is depicted in Figure 31.
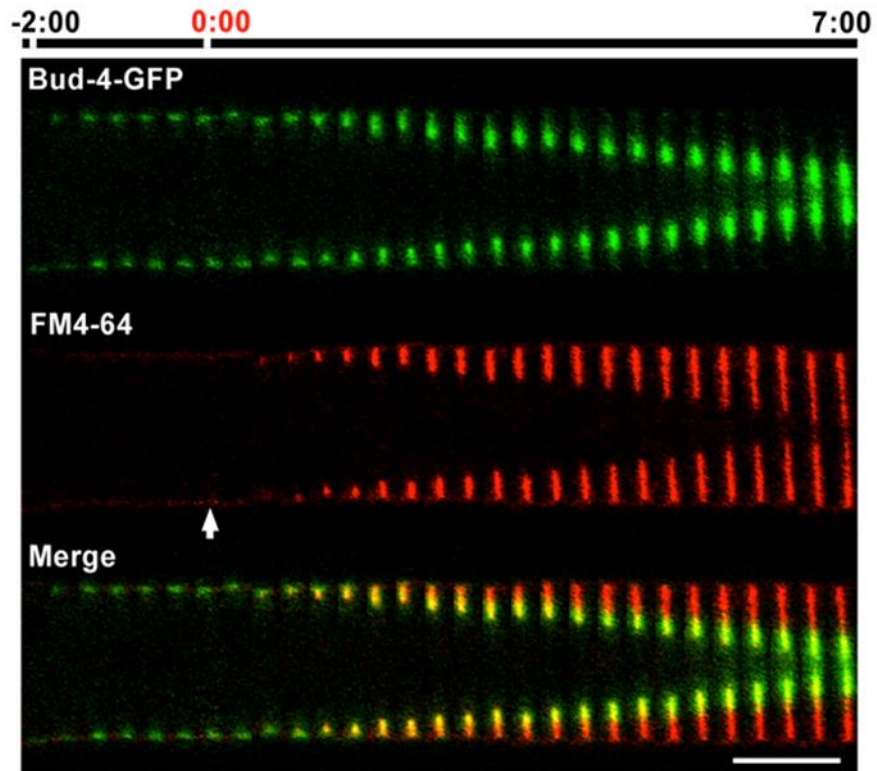
Figure 29: Chronology of Bud-4 in septum development. Series constructed from images taken at 20 sec intervals and assembled to emulate kymographs. BUD-4 colocalizes only the leading edge of the growing plasma membrane. Time 0:00 (arrows) signals the earliest moment of membrane invagination. Scale bar = 5 μm.
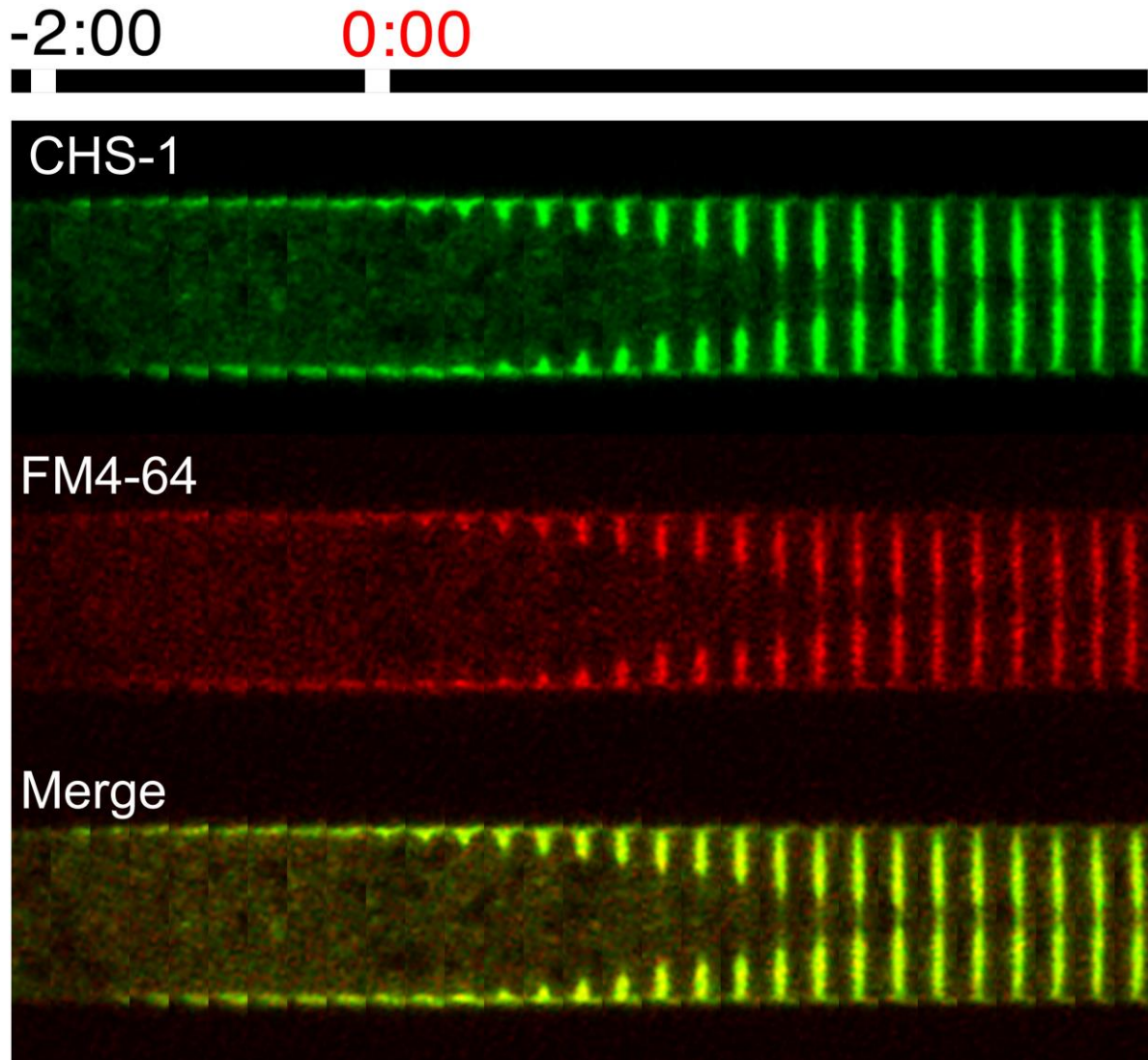
Figure 21: Chronology of Chitin synthase 1 (CHS-1) in septum development. Series constructed from images taken at 20 sec intervals and assembled to emulate kymographs. CHS-1-GFP expressed under its native promoterTime 0:00 (arrows) signals the earliest moment of membrane invagination. Scale bar = 5 μm.

Figure 31: The timing of events that lead to septum formation. The events that lead to septum formation are featured in columns. The timing at which a protein appears at each event is pictured as a red line.

4.5.2.6 Septa are formed at regular intervals in leading N. crassa hyphae

Septum formation occurred at interval lengths of 93 ± 2 µm (mean ± standard error) (n=36) along the hyphal tube (Fig 32. Movie 12). When the apical compartment (the segment between the tip and its nearest septum) reached a critical length (250 ± 5 µm; n=10) a new septum started to develop. The distance from the apex to the new septation site was 166 ± 3 µm (n=50); septation splits the leading hyphal compartment into two unequal segments, the apical one being 2.5X longer (Fig. 32). Figure 32 shows the spatiotemporal regularity of septation. Septum formation occurred without affecting the apical growth rate (13 µm min^{-1}) (Fig. 32D). Above measurements where made from time-series of *N. crassa* tagged with Lifeact (Movie 12).
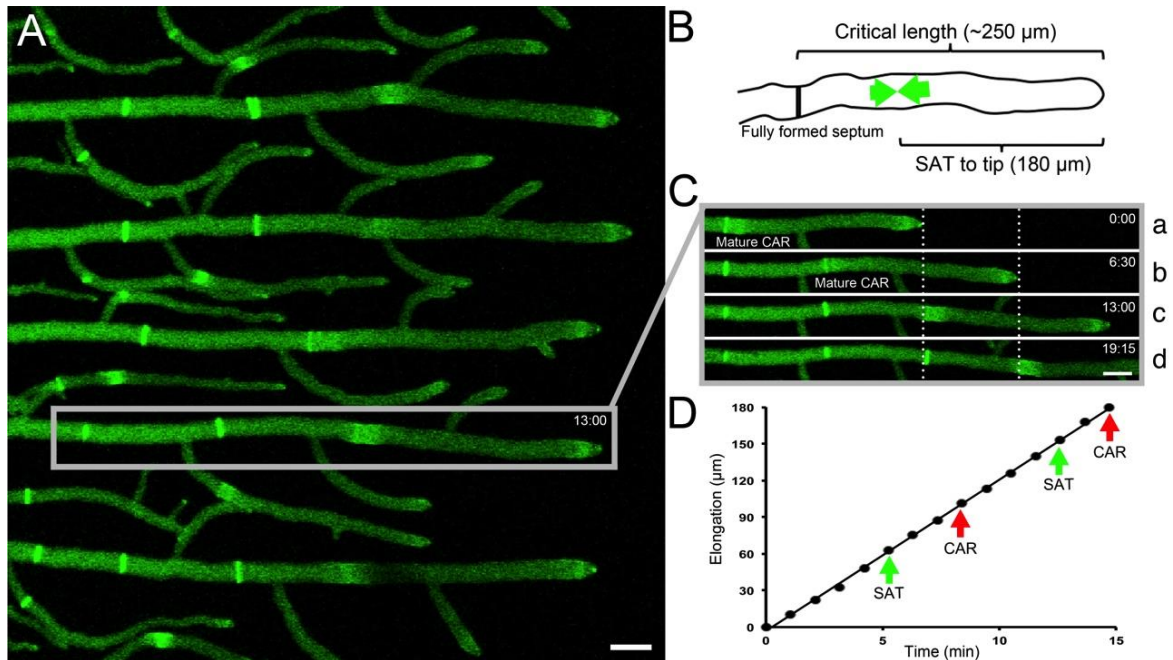
Figure 32: Septum development in hyphae of *Neurospora crassa* visualized by fluorescent tagging of actin with Lifeact-GFP. (A) Growth of primary hyphae monitored for up to 20 min. Lifeact-GFP fluorescence reveals the presence of actin in septa (s), septal actomyosin tangles (t), subapical collars (c) and Spitzenkörper (k). (B) Critical hyphal dimensions for septation. As a hypha reaches a critical length of ~250 μm from the last septation site, a new SAT begins to assemble (green arrows) at the future septation site located at about 180 μm from the tip. (C) Stages in the septation of a single hypha. The dotted lines mark the position of the tip at two consecutive times and, predictably, the place where septation occurred ~ 6 min later. (D) Kinetics of hyphal elongation and timing of two SAT and CAR events. Note septum formation did not affect the apical growth rate. Scale Bar = 10 μm.

Chapter 5: Discussion

5.1 Development of functional live actin reporters: full-length proteins and truncated versions.

In this study, we describe a set of in vivo F-actin reporters that have proven useful for the study of the actin cytoskeleton in *N. crassa*. We used the ABPs fimbrin, tropomyosin, ARP-2, ARP-3, and Lifeact (Riedl et al., 2008), all fused to the N-terminus of GFP and/or mChFP as reporters for actin distribution. The truncated version of fimbrin (Abd2) is a good reporter as the full-length protein, because it displayed the same distribution and dynamics. It retained the ability to bind to a specific population of actin filaments found in the cell cortex, similar to what has been shown in *Arabidopsis thaliana* root hairs (Sheahan et al., 2004; Wang et al., 2004a), Our findings extend recent observations made with live cell actin markers in *A. nidulans* germlings (Upadhyay and Shaw, 2008; Taheri-Talesh et al., 2008; Araujo-Bazán et al., 2008) by analyzing actin dynamics in mature hyphae, emerging branches and developing septa of *N. crassa*. We found that different ABPs labeled different subsets of actin structures, and we also identified a global marker for F-actin in this fungus (Lifeact).

The actin binding peptide Lifeact (Riedl et al., 2008) was successfully expressed in *N. crassa*, revealing the two main actin populations in the fungal cell:patches and cables. Lifeact has been shown to successfully label actin in many other organisms besides the fungal kingdom (Riedl et al., 2008).

Table 3: Localization of actin cytoskeleton reporters.

Reporter	Structure	Localization
Abd-2-GFP	Patches	Subapical cortical collar Cortical all throughout the cell Developing septa
ARP-2-GFP	Patches	Subapical collar Cortical all throughout the cell Developing septa
Tropomyosin	Spitzenkörper aggregation Cables	Tip Subapical cortical Future septation sites
Lifeact	Patches Spitzenkörper aggregation Cables	Subapical cortical collar Cortical all throughout the cell Future septation sites
Myosin (class II)	Cables	Future septation sites Septal Actomyosin Tangle Contractile Actomyosin Ring

5.2 Actin exists in different structural states (or configurations) in the hyphal cell

Actin is found in different configurations in the hyphal cell. The labeling of actin with functional live actin reporters (Actin binding proteins) allowed for the determination of the structural state of the actin cytoskeleton in the different regions of the cell.

5.2.1 Apical actin organizes the Spk

The findings on the localization of tropomyosin and Lifeact in the Spk are consistent with previous descriptions of actin in different fungi based on immuno-staining methods (Bourett and Howard, 1991; Srinivasan et al., 1996; Heath et al., 2000; Virag and Griffiths, 2004) and live-cell imaging using ABPs labeled with fluorescent proteins (Taheri-Talesh et al., 2008). Discrete cables of F-actin were not observed in the Spk. Indeed, reports based on TEM describe F-actin organization as a dense meshwork in which other components of the Spk are embedded (Howard, 1981; Roberson and Fuller, 1988; Roberson et al., 2010). Contractile forces within the Spk are needed not only to maintain its order, but also to promote movement. The spatial distribution of Spk elements is maintained throughout apical growth (Sharpless and Harris, 2002; Harris et al., 2005; Li et al., 2006). The findings reported here are consistent with F-actin serving as the scaffold that regulates the distribution and motility of Spk components, which results in the efficient control of the tip growth apparatus. This idea is supported by the finding that the polarisome and the Spk are disassembled following treatment with latrunculin or cytochalasin (Araujo-Palomares et al., 2009). Tropomyosin may well be the protein for this function, as it has been shown to regulate the contact between F-actin and myosins, and also to stabilize actin filaments (Pittenger et al., 1994; Dos Remedios et al., 2003).

5.2.2 Subapical actin patches aid endocytosis

In the subapex, F-actin was found as a cortical ring of patches labeled by fimbrin, ARP3, and Lifeact. These actin patches closely resemble the actin structures revealed by rhodamine-phaloidin labeling in S. cerevisiae (Adams and Pringle, 1981) and immunolocalization with anti-actin antibodies in the filamentous fungi *N. crassa* (Heath et al., 2000), *Sclerotium rolfsii* (Roberson, 1992), *Allomyces macrogynus* (Srinivasan et al., 1996) and *Mucor rouxii* (Hasek and Bartnicki-Garcia, 1994). In living germlings of *A. nidulans*, actin patches were labeled by FimA:GFP and ActA:GFP (Upadhyay and Shaw, 2008). In *N. crassa*, abundant actin patches were localized throughout the cell cortex. TIRFM demonstrated an abundance of cortical patches in the basal region of hyphae, which would have been difficult, to ascertain by confocal microscopy, due to resolution limitations. F-actin patches were most abundant in the subapical region, which has been referred to as the endocytic zone (Upadhyay and Shaw, 2008; Araujo-Bazán et al., 2008). This accumulation is consistent with their known role in endocytosis in S. cerevisiae, *A. nidulans* and *A. oryzae*. In S. cerevisiae studies of Sac6 (fimbrin) null mutants revealed severe defects in the endocytic uptake of a-factor, demonstrating that fimbrin is essential for endocytosis (Kübler and Riezman, 1993; Geli and Riezman, 1998). In addition, Sac6 labeled with GFP co-localized with the endocytic marker FM4-64 (Huckaba et al., 2004). Similar to our findings, actin patches are resistant to depolymerization by anti-actin drugs in *S. cerevisiae*. Actin patches purified from a wild type strain of *S. cerevisiae* are resistant to actin

depolymerization, whereas patches purified from *sac6*D mutants are highly susceptible to anti-actin drugs, demonstrating that fimbrin stabilizes actin patches *in vitro* (Young et al., 2004). Therefore we propose that the actin patches observed in *N. crassa* correspond to sites of endocytosis as they do in other fungi. A second type of F-actin array was found in the hyphal sub-apex tagged by tropomyosin-GFP and Lifeact-GFP, forming cables exclusively in the cell cortex. cytoplasmic cables were not detected, tagged either by tropomyosin-GFP or Lifeact-GFP, as reported in *A. nidulans* germlings (Taheri-Talesh et al., 2008). Surprisingly, in *A. nidulans* the G-actin reporter (ActA:GFP) (Taheri-Talesh et al., 2008; Upadhyay and Shaw, 2008) does not label the actin cables.

5.2.3 TIRFM reveals antero- and retrograde actin patch movement

To extend our observations of patch behavior we used TIRFM, a technique that allows the visualization of fluorophores close to the specimen/cover glass interphase. TIRFM also allows higher temporal resolution, lower photobleaching and significantly reduces background fluorescence. The high temporal resolution allowed assessment the motility of cortical patches. We found that in *N. crassa*, patch movement can be either anterograde or retrograde as has been observed in *S. cerevisiae*, *S. pombe* (Pelham and Chang, 2001; Smith et al., 2001; Carlsson et al., 2002; Huckaba et al., 2004) and *A. nidulans* (Upadhyay and Shaw, 2008). As demonstrated in *S. cerevisiae* (Huckaba et al., 2004) and in *S. pombe* (Pelham and Chang, 2001), patch movement at the surface plane in *N. crassa* was F-actin cable dependent, since treatment with latrunculin and cytochalasin stopped patch

movement. The actin patch speed measured in *N. crassa* (3.35 lm s^{-1}) is the highest reported for fungal cells, an order of magnitude higher than those reported for *A. nidulans* (0.19–0.56 lm s^{-1}) (Upadhyay and Shaw, 2008) or the yeasts *S. cerevisiae* (0.31 lm s^{-1}) and *S. pombe* (0.3 lm s^{-1}) (Waddle et al., 1996; Carlsson et al., 2002). While patches move at high speed, the patch lifetime in *N. crassa* (5.2 s) was significantly shorter than those reported for *A. nidulans* or *S. cerevisiae*. AbpA-labeled patches in *A. nidulans* have an average lifetime of 24 s (Araujo-Bazán et al., 2008) and Abp1-labeled patches in *S. cerevisiae* had an average lifetime of about 15 s (Huckaba et al., 2004). The difference in lifetime measurements may be related to the microscopy technique used in each case. Our study employed TIRFM where the optical slice is ~100 nm, whereas with other techniques including confocal microscopy the smallest optical slice is 700 nm. Thus, TIRFM allows more accurate determination of the timing of patch dissociation from the plasma membrane.

5.3 ABPs form distinct rings during septum formation

Despite the importance of septum formation for growth and differentiation of filamentous fungi, which resemble the majority of the fungal kingdom, our understanding of septum formation and its regulation in filamentous fungi is highly fragmentary. Septum formation is regulated in two stages; A) the post-mitotic kinases of the SIN cascade and B) the *in situ* process of cross wall construction. Many of the proteins involved in each stage of septation have been identified; although the main mechanisms seem to be conserved between yeast and

filamentous fungi (Chant and Pringle, 1991; Bulawa, 1993; Momany et al., 1995; Seiler and Justa-Schuch, 2010), there are some important differences. Most work on septation in filamentous fungi has been done with *A. nidulans* (Momany et al., 1995; Harris, 2001). For *N. crassa*, there are reports on specific components of the septation process (Seiler and Justa-Schuch, 2010; Mouriño-Pérez, 2013; Mouriño-Pérez and Riquelme, 2013). This is the first comprehensive attempt to define the sequence of key events in septum formation in *N. crassa* (Fig. 6 and 7). The work focused in the processes that occur in the septation site, analyzing the timing of the different proteins involved in septal development from the initiation to the final construction, including the markers that determine the septation site (i.e. cell division plane). The actin reporter Lifeact-GFP was used (Delgado-Alvarez et al., 2010; Berepiki et al., 2010) and we found that it is a bona fide marker of actin involvement throughout the entire process of septum formation.

The precise development of a new septum at a defined position ca. 165 µm subapically of the growing tip of mature hyphae, strongly suggests a size-sensing mechanism for determining septation sites. Nuclear position and cell cycle is one determinant of septum placement in *A. nidulans* (and possibly also *N. crassa*), not every nuclear division is triggering the formation of a septum (Harris, 2001; Gladfelter, 2006). The impact of nuclear position and cell cycle progression in determining this site is currently unclear and will be a major focus of future work. The SIN is essential for septum formation in yeasts and filamentous fungi (Hachet and Simanis, 2008; Seiler and Justa-Schuch, 2010) and is thus a prime candidate for connecting cell cycle with septum placement. However, no evidence for a

mechanistic involvement of the SIN in connecting both events does currently exist in filamentous fungi (Kim et al., 2009; Heilig et al., unpublished).

Although it may be expected that proteins involved in the post-mitotic signals of the SIN cascade (Seiler and Justa-Schuch, 2010) are the first to appear at the septation site, in *N. crassa* we have identified an F-actin network as the earliest component in the selection of the site of septation in the form of a tangle of thick cables (SAT) associated to tropomyosin and a Class II myosin. This actomyosin structure is visible around five min before any other visible sign of septation. A study about SIN components in *N. crassa*, showed that DBF-2 was previously shown to reach the septation site around two min before plasma membrane ingrowth in *N. crassa* (Heilig et al., unpublished), too late to be the signal driving the actomyosin components to form the SAT. Hence, the signal previous to SAT formation remains unknown.

The SAT coalesces and is transformed into a contractile ring without the presence of the formin BNI-1 and the BUD-4/BUD-3/RHO-4 complex that are essential for septum formation (Justa-Schuch et al., 2010; Seiler and Justa-Schuch, 2011, Heilig et al., unpublished). Therefore, formin- and anillin-dependent F-actin nucleation and organization seems to be not important for SAT formation. Nevertheless, the appearance of BUD-4 and BNI-1 coincides with the maturation of the CAR from the proto-CAR and must have a critical role for its constriction. A new SAT may primarily be generated by transferring existing filaments from a previously established septum. It is currently unclear if this transfer is based on treadmilling of filaments or on myosin-dependent transport of F-actin.

During SAT and CAR establishment, actin binding proteins delimit the structure and provide the machinery needed for its coalescence and later constriction. The myosin MYO-2, provides the contractile force for SAT and CAR. MYO-2 appears in early stages of SAT formation aligned with the Lifeact-GFP labeled cables. Tropomyosin is a protein that regulates the interaction between actin filaments and myosin (Balasubramanian et al., 1992; Pollard, 2008). It was shown to be associated with the early stages of SAT formation. This protein seems to be a permanent resident of the actin filaments that travels from one septum to another and polymerizes and organizes in unison with the actin cables in the SAT.

The conversion of the SAT into the actual CAR in *N. crassa* resembles the process previously described in *S. pombe* (Lord, 2010; Kovar et al., 2011). The process of SAT formation and transformation to CAR has been called the "search, capture, pull, and release" (SCPR) model (reviewed in Lord, 2010). However, there are some differences in SAT formation between *S. pombe* and *N. crassa*. The first difference is the accumulation of the anillin-like Mid1 nodes in the division site almost one hour before mitosis in *S. pombe* (Chang et al., 1997; Sohrmann et al., 1996; Bahler et al., 1998). Close to the beginning of mitosis, Mid1 recruits a broad band of nodes containing a Class II myosin (Myo2), and its two light chains Cdc4 and Rlc1, formin (Cdc12) and tropomyosin (Cdc8) (Wu et al., 2003, 2006; Pollard, 2008; Vavylonis et al., 2008; Coffman et al., 2009). In *N. crassa* there is no Mid1 homologue, and no other known protein forms nodes close to the septation site with this timing. However, Myo2 is present a few minutes before any sign of plasma membrane ingrowth following the profile of the forming actin filaments. In

S. pombe, formin nucleates actin filaments that associate with tropomyosin to initiate the septation process. In *N. crassa* formin plays a role when the CAR is established but not during the initial organization of actin filaments (SAT).

We followed the incorporation of chitin synthase, CHS-1, into the septation process as a representative of the exocytic events that deliver wall building enzymes to the septum. It should be noted that *N. crassa* contains not one but seven chitin synthases and all have been found to travel to the septation sites (Riquelme et al., 2007; Sanchez-León et al., 2011; Fajardo-Somera et al., 2013). Localization of multiple chitin synthases at septa has been also reported in other fungi (Motoyama et al., 1994, 1996; Fujiwara et al., 1997; Ichinomiya et al., 2002, 2005; Takeshita et al., 2005, 2007; Yamada et al., 2005; Horiuchi, 2009; Weber et al., 2006).

The fusion of vesicles carrying cell wall precursors to the plasma membrane in the septation site produces a simultaneous growth of both (cell wall and plasma membrane). There is no plasma membrane invagination *sensu stricto*; it is new membrane growing in a centripetal manner. Calculations on the amount of plasma membrane generated during apical cell wall growth indicate that an excess of membrane is produced that needs to be removed (Bartnicki-García, unpublished). The latter would probably depend on the same machinery that functions during endocytosis in other parts of the cell. A supposition supported by the finding of actin patches containing fimbrin, Arp2/3 complex and coronin; proteins associated with endocytic function (Delgado-Alvarez et al., 2010; Echauri-Espinosa et al., 2012).

5.4 Function of actin structures

Actin is one of the most abundant proteins in eukaryotes and plays a major role in diverse cellular functions. The associations of actin with other proteins in filamentous fungi are not well understood. Reliable reporters for the complete actin population and its various subsets are needed in order to address some of the key questions about actin function in polarized growth and development. Here, different actin reporters were evaluated, that together label a wide range of actin arrays in mature hyphae of *N. crassa*. Each array is associated with particular actin-binding proteins that presumably participate in the regulation of its localization, dynamics and function.

Chapter 6: Conclusions

- Truncated protein reporters of actin are as reliable as full-length protein reporters.

- The identity of actin populations is dependent of the actin binding proteins. ABPs determine the three dimensional structure of the actin cytoskeleton

- Linear actin cables, stabilized by tropomyosin, play a role in long distance movement of vesicles.

- The patch configuration (subapical collar), composed of short filaments, branched by the Arp2/3 complex, and bundled by Fimbrin (among other proteins) participates in endocytosis.

- Actin and tropomyosin are components of actomyosin complex present in the Spitzenkörper.

- Actin in the subapex is organized as cortical cables and cortical patches.

- Septum formation is a growth event that is not that different from the tip.

- Septum formation follows a morphogenetic pattern.

- In a chronological manner, the steps to form a septum include: 1) accumulation of a broad band of actin surrounding the future septation site (SAT), 2) endowment of F-actin with a contractile force through recruitment of Myo2, 3)

establishment of the exact location for CAR formation, 4) constriction of the CAR, 5) invagination and remodeling of plasma membrane coupled with 6) construction of the cell wall.

References

Adams, A. E., Botstein, D. & Drubin, D. G. (1991). Requirement of yeast fimbrin for actin organization and morphogenesis in vivo. Nature. 354:404-408.

Adams, A. E., Pringle, J. R. (1981). Relationship of actin and tubulin distribution to bud growth in wild-type and morphogenetic-mutant *Saccharomyces cerevisiae.* J. Cell Biol. 98:934-945.

Arai, R., Nakano, K. & Mabuchi, I. (1998). Subcellular localization and possible function of actin, tropomyosin and actin-related protein 3 (Arp3) in the fission yeast *Schizosaccharomyces pombe.* Eur. J. Cell Biol. 76:288-295.

Araujo-Bazán, L., Peñalva, M. A. & Espeso, E.A. (2008). Preferential localization of the endocytic internalization machinery to hyphal tips underlies polarization of the actin cytoskeleton in *Aspergillus nidulans.* Mol. Microbiol. 67:891-905.

Araujo-Palomares, C. L., Riquelme, M. & Castro-Longoria, E. (2009). The polarisome component SPA-2 localizes at the apex of *Neurospora crassa* and partially co-localizes with the Spitzenkörper. Fungal Genet. Biol. 46:551-563.

Axelrod, D. (2001). Total internal reflection fluorescence microscopy in cell biology. Traffic 2:764-774

Ayscough, K. R. (2005). Coupling actin dynamics to the endocytic process in *Saccharomyces cerevisiae.* Protoplasma. 226:81-88.

Bahler, J., Steever, A. B., Wheatley, S., Wang, Y. L., Pringle, J. R., Gould, K. L., & McCollum, D. (1998). Role of polo kinase and Mid1p in determining the site of cell division in fission yeast. J Cell Biol. 143:1603-1616.

Balasubramanian, M. K., Helfam, D. M., Hemmingsen, S. M., (1992) A new tropomyosin essential for cytokinesis in the fission yeast *S. pombe*. Nature 360:84-87.

Bartnicki-García, S. (2002). Hyphal tip growth: outstanding questions. In Molecular biology of fungal development. Osiewacz, H. D. (ed). CRC Press, pp. 29-58.

Bartnicki-Garcia, S., Lippman, E. (1977). Polarization of cell wall synthesis during spore germination of Mucor rouxii. Exp Mycol 1:230-240.

Berepiki, A., Lichius, A., & Read, N. D. (2011). Actin organization and dynamics in filamentous fungi. Nat Rev Microbiol 9:876-887.

Bezanilla, M., Wilson, J. M. & Pollard, T. D. (2000). Fission yeast myosin-II isoforms assemble into contractile rings at distinct times during mitosis. Curr. Biol. 10:397-400.

Bi, E., Maddox, P., Lew, D. J., Salmon, E. D., McMillan, J. N., Yeh, E. & Pringle, J. R. (1998). Involvement of an actomyosin contractile ring in *Saccharomyces cerevisiae* cytokinesis. J. Cell Biol. 142:1301-1312.

Bourett, T. M., Howard, R. J. (1991). Ultrastructural immunolocalization of F-actin in a fungus. Protoplasma. 163:199-202.

Bracker, C.E. (1967). Ultrastructure of fungi. Annu Rev Pytopathol 5:343-374.

Bretscher, A. (2003). Polarized growth and organelle segregation in yeast:the tracks, motors, and receptors. J. Cell Biol. 160:811-816.

Bulawa, C.E. (1993). Genetics and molecular biology of chitin synthesis in fungi. Annu Rev Microbiol 47:505-534.

Calvert, M. E. K., Wright, G. D., Leong, F. Y., Chiam, K-H., Chen, Y., Jedd, G. & Balasubramanian, M. K. (2011). Myosin concentration underlies cell size-dependent scalability of actomyosin ring constriction. J Cell Biol 195:799-813.

Carlsson, A. E., Shah, A. D., Elking, D., Karpova, T. S. & Cooper, J. A. (2002). Quantitative analysis of actin patch movement in yeast. Biophys. J. 82:2333-2343.

Chang F, Nurse P. (1997). cdc12p, a protein required for cytokinesis in fission yeast, is a component of the cell division ring and interacts with profilin. J Cell Biol 137:169-182.

Chant, J., Pringle, J. R. (1970). Budding and cell polarity in *Saccharomyces cerevisiae*. Curr Opin Genet Dev 1:342-350.

Clutterbuck, A. J. (1970) Synchronous nuclear division and septation in *Aspergillus nidulans.* J Gen Microbiol 60:133-135.

Coffman, V.C., Nile, A. H., Lee, I. J., Liu, H., & Wu, J. Q. (2009). Roles of formin nodes and myosin motor activity in Mid1p-dependent contractile-ring assembly during fission yeast cytokinesis. Mol Biol Cell 20:5195-5152-5110.

Davis, R. H. (2000). Neurospora, Contributions of a Model Organism. Oxford University Press..333p.

De Arruda, M. V., Watson, S., Lin, C. S., Leavitt, J. & Matsudaira, P. (1990). Fimbrin is a homologue of the cytoplasmic phosphoprotein plastin and has domains homologous with calmodulin and actin gelation proteins. J. Cell Biol. 111:1069-1079.

Delgado-Alvarez, D. L., Callejas-Negrete, O. A., Gómez, N., Freitag, M., Roberson, R. W., Smith, L. G., & Mouriño-Pérez, R. R. (2010). Visualization of F-actin localization and dynamics with live cell markers in *Neurospora crassa*. Fungal Genet Biol 47:573-586.

Dos Remedios, C. G., Chhabra, D., Kekic, M., Dedova, I. V., Tsubakihara, M., Berry, D. A. & Nosworthy, N. J. (2003). Actin binding proteins:regulation of cytoskeletal microfilaments. Physiol. Rev. 83:433-473.

Echauri-Espinosa, R. O., Callejas-Negrete, O. A., Roberson, R. W., Bartnicki-Garcia, S. & Mourino-Perez, R. R. (2012). Coronin is a component of the endocytic collar of hyphae of *Neurospora crassa* and is necessary for normal growth and morphogenesis. PLoS One 7:e38237.

Eggert, U. S., Kiger, A. A., Richter, C., Perlman, Z. E., Perrimon, N., Mitchison, T. J. & Field, C. M. (2004). Parallel chemical genetic and genome-wide RNAi screens identify cytokinesis inhibitors and targets. PLoS Biol. 2, e379.

Egile, C., Rouiller, I., Xu, X., Volkmann, N., Li, R. & Hanein, D. (2005). Mechanism of filament nucleation and branch stability revealed by the structure of the Arp2/3 complex at actin branch junctions. PLoS Biol. 3, e383.

Fajardo-Somera, R. A., Roberson, R. W., Johnk, B., Bayram, O., Braus, G. H., & Riquelme, M. (2013). The role and traffic of chitin synthases in *Neurospora crassa*. Presented in the 27th Fungal Genetics Conference. Pacific Grove, California, USA.

Fiddy, C., Trinci, A. P. J. (1976). Mitosis, septation, branching and the duplication cycle in *Aspergillus nidulans*. J Gen Microbiol 97:169-184.

Fischer-Parton, S., Parton, R. M., Hickey, P. C., Dijksterhuis, J., Atkinson, H. A., & Read, N. D. (2000) Confocal microscopy of FM4-64 as a tool for analyzing endocytosis and vesicle trafficking in living fungal hyphae. J Microsc 198:246-259.

Fleissner, A., Sarkar, S., Jacobson, D. J., Roca, M. G., Read, N. D., & Glass, N. L. (2005). The so locus is required for vegetative cell fusion and postfertilization events in *Neurospora crassa*. Eukaryot Cell 4:920-930.

Freitag, M., Hickey, P. C., Raju, N. B., Selker, E. U. & Read, N. D., (2004). GFP as a tool to analyze the organization, dynamics and function of nuclei and microtubules in *Neurospora crassa*. Fungal Genet. Biol. 41:897-910.

Fujiwara, M., Horiuchi, H., Ohta, A., & Takagi, M. (1997). A novel fungal gene encoding chitin synthase with a myosin motor-like domain. Biochem Biophys Res Commun 236:75-78.

Gachet, Y., Hyams, J. S. (2005). Endocytosis in fission yeast is spatially associated with the actin cytoskeleton during polarised cell growth and cytokinesis. J. Cell. Sci. 118:4231-4242.

Geli, M. I., Riezman, H. (1998). Endocytic internalization in yeast and animal cells:similar and different. J. Cell. Sci. 111 (Pt 8):1031-1037.

Gladfelter, A. S. (2006). Nuclear anarchy:asynchronous mitosis in multinucleated fungal hyphae. Curr Opin Microbiol 9:547-552.

Greenberg, M. J., Wang, C. A., Lehman, W. & Moore, J. R. (2008). Modulation of actin mechanics by caldesmon and tropomyosin. Cell Motility and the Cytoskeleton. 65:156-164.

Gregory, P. H. (1984). The fungal mycelium an historical persp. In The Ecology and physiology of the fungal mycelium. Jennings, D. H., and Rayner, A. D. M. (ed):Cambridge University Press, pp. 1-22.

Gull, K. (1978). Form and Function of Septa in Filamentous Fungi. In The filamentous Fungi. Vol. III. Smith, J. E., and Berry, D. R. (ed). London:Edward Arnold., pp. 78-93.

Hachet, O., Simanis, V. (2008) Mid1p/anillin and the septation initiation network orchestrate contractile ring assembly for cytokinesis. Genes Dev 22:3205-3216.

Harris, S. D. (2001) Septum formation in *Aspergillus nidulans*. Curr Opin Microbiol 4:736-739.

Harris, S. D. (2011). Hyphal morphogenesis:an evolutionary perspective. Fungal Biol Rev 115:475-484.

Harris, S. D., Hamer, L., Sharpless, K. E., Hamer, J. E. (1997). The *Aspergillus nidulans* sepA gene encodes an FH1/2 protein involved in cytokinesis and the maintenance of cellular polarity. Embo J. 16:3474-3483.

Harris, S. D., Momany, M. (2004). Polarity in filamentous fungi:moving beyond the yeast paradigm. Fungal Genet. Biol. 41:391-400.

Harris, S. D., Morrell, J. L., & Hamer, J. E. (1994). Identification and characterization of *Aspergillus nidulans* mutants defective in cytokinesis. Genet 136:517-532.

Harris, S. D., Read, N. D., Roberson, R. W., Shaw, B., Seiler, S., Plamann, M. & Momany, M. (2005). Polarisome meets spitzenkörper:microscopy, genetics, and genomics converge. Eukaryotic Cell. 4:225-229.

Hasek, J., Bartnicki-Garcia, S. (1994). The arrangement of F-actin and microtubules during germination of *Mucor rouxii* sporangiospores. Arch. Microbiol. 161:363-369.

Heath, I. B., Gupta, G. & Bai, S. (2000). Plasma membrane-adjacent actin filaments, but not microtubules, are essential for both polarization and hyphal tip morphogenesis in *Saprolegnia ferax* and *Neurospora crassa*. Fungal Genet. Biol. 30:45-62.

Hernández-Rodríguez, Y., Hastings, S., & Momany, M. (2012). The Septin AspB in *Aspergillus nidulans* Forms Bars and Filaments and Plays Roles in Growth Emergence and Conidiation. Eukaryot Cell 11:311-323.

Hickey, P. C., Jacobson, D., Read, N. D. & Glass, N. L. (2002). Live-cell imaging of vegetative hyphal fusion in *Neurospora crassa*. Fungal Genet. Biol. 37:109-119.

Horiuchi, H. (2009). Functional diversity of chitin synthases of *Aspergillus nidulans* in hyphal growth, conidiophore development and septum formation. Med Mycol 47:S47-S52. doi:10.1080/13693780802213332

Howard, R. J. (1981). Ultrastructural analysis of hyphal tip cell growth in fungi:Spitzenkörper, cytoskeleton and endomembranes after freeze-substitution. J. Cell. Sci. 48:89-103.

Huckaba, T. M., Gay, A. C., Pantalena, L. F., Yang, H. & Pon, L. A. (2004). Live cell imaging of the assembly, disassembly, and actin cable-dependent movement of endosomes and actin patches in the budding yeast, *Saccharomyces cerevisiae*. J. Cell Biol. 167:519-530.

Ichinomiya, M., Yamada, E., Yamashita, S., Ohta, A., & Horiuchi, H. (2005). Class I and class II chitin synthases are involved in septum formation in the filamentous fungus *Aspergillus nidulans*. Eukaryot Cell 4:1125-1136.

Jedd, G., Chua, N-H. (2000). A new self-assembled peroxisomal vesicle required for efficient resealing of the plasma membrane. Nature Cell Biology 2:226-231.

Justa-Schuch, D., Heilig, Y., Richthammer, C., & Seiler, S. (2010). Septum formation is regulated by the RHO4-specific exchange factors BUD3 and RGF3 and by the landmark protein BUD4 in *Neurospora crassa*. Mol Microbiol 76:220-235.

Kaksonen, M., Sun, Y. & Drubin, D. G. (2003). A pathway for association of receptors, adaptors, and actin during endocytic internalization. Cell. 115:475-487.

Kaksonen, M., Toret, C. P. & Drubin, D. G. (2005). A modular design for the clathrin- and actin-mediated endocytosis machinery. Cell. 123:305-320.

Kamasaki, T., Osumi, M., & Mabuchi, I. (2007). Three-dimensional arrangement of F-actin in the contractile ring of fission yeast. J Cell Biol 178:765-771.

Kim, J. M., Zeng, C. J., Nayak, T., Shao, R., Huang, A. C., Oakley, B. R., & Liu, B. (2009). Timely septation requires SNAD-dependent spindle pole body localization of the septation initiation network components in the filamentous fungus *Aspergillus nidulans*. Mol Biol Cell 20:2874-2884.

King, S. B. Alexander, L. J. (1969). Nuclear behavior, septation and hyphal growth of *Alternaria solani*. Am J Bot 56:249-253.

Kovar, D. R., Sirotkin, V., & Lord, M. (2011). Three's company:the fission yeast actin cytoskeleton. Trends Cell Biol 21:177-187.

Kübler, E., Riezman, H. (1993). Actin and fimbrin are required for the internalization step of endocytosis in yeast. Embo J. 12:2855-2862.

Li, S., Du, L., Yuen, G. & Harris, S. D. (2006). Distinct ceramide synthases regulate polarized growth in the filamentous fungus *Aspergillus nidulans*. Mol. Biol. Cell. 17:1218-1227.

Lichius, A., Yáñez-Gutiérrez, M. E., Read, N. D. & Castro-Longoria, E. (2012). Comparative live-cell imaging analyses of SPA-2, BUD-6 and BNI-1 in *Neurospora crassa* reveal novel features of the filamentous fungal polarisome. PLoS ONE 7:e30372.

Liu, F., Ng, S. K., Lu, Y., Low, W., Lai, J. & Jedd, G. (2008). Making two organelles from one:Woronin body biogenesis by peroxisomal protein sorting. J Cell Biol 180:325-339.

Lord, M. (2010). Cytokinesis mechanisms in yeast. Nature Education 3:53.

Margolin, B. S., Freitag, M. & Selker, E. U. (1997). Improved plasmids for gene targeting at the his-3 locus of *Neurospora crassa* by electroporation. Fungal Genet. Newslett. 44, 34–36 correction. Fungal Genet. Newslett. 47:112.

Martin, S. G. (2009). Microtubule-dependent cell morphogenesis in the fission yeast. Trends Cell Biol 19:447-454.

McCollum, D., Feoktistova, A., Morphew, M., Balasubramanian, M. & Gould, K. L. (1996). The *Schizosaccharomyces pombe* actin-related protein, Arp3, is a component of the cortical actin cytoskeleton and interacts with profilin. Embo J. 15:6438-6446.

McDaniel, D. P., Roberson, R. W. (2000). Microtubules are required for motility and positioning of vesicles and mitochondria in hyphal tip cells of *Allomyces macrogynus*. Fungal Genet. Biol. 31:233-244.

McGoldrick, C. A., Gruver, C. & May, G. S. (1995). myoA of *Aspergillus nidulans* encodes an essential myosin I required for secretion and polarized growth. J. Cell Biol. 128:577-587.

Minke, P. F., Lee, I. H., & Plamann, M. (1999). Microscopic analysis of Neurospora ropy mutants defective in nuclear distribution. Fungal Genet Biol 28:55-67.

Momany, M., Morrell, J. L., Harris, S. D. & Hamer, J. E. (1995). Septum formation in *Aspergillus nidulans*. Can. J. Bot. 73:396-399.

Momany, M., Hamer, J. E. (1997b). The *Aspergillus nidulans* Septin Encoding Gene, aspB, Is Essential for Growth. Fungal Genet Biol 21:92-100.

Momany, M., Hamer, J.E. (1997a). Relationship of Actin, Microtubules, and Crosswall Synthesis During Septation in *Aspergillus nidulans*. Cell Mot Cytoskel 38:373-384.

Momany, M., Morrell, J. L., Harris, S. D., & Hamer, J. E. (1995). Septum formation in *Aspergillus nidulans*. Can J Bot 73:S396-S399.

Momany, M., Taylor, I. (2000). Landmarks in the early duplication cycles of *Aspergillus fumigatus* and *Aspergillus nidulans*:polarity, germ tube emergence and septation. Microbiol 146:3279-3284.

Moseley, J. B., Goode, B. L. (2006). The yeast actin cytoskeleton:from cellular function to biochemical mechanism. Microbiol. Mol. Biol. Rev. 70:605-645.

Motegi, F., Mishra, M., Balasubramanian, M. K. & Mabuchi, I. (2004). Myosin-II reorganization during mitosis is controlled temporally by its dephosphorylation and spatially by Mid1 in fission yeast. J. Cell Biol. 165:685-695.

Motegi, F., Nakano, K. & Mabuchi, I. (2000). Molecular mechanism of myosin-II assembly at the division site in *Schizosaccharomyces pombe.* J. Cell. Sci. 113 (Pt 10):1813-1825.

Motoyama, T., Fujiwara, M., Kojima, N., Horiuchi, H., Ohta, A., & Takagi, M. (1997). The Aspergillus nidulans genes chsA and chsD encode chitin synthases which have redundant functions in conidia formation. Mol Gen Genet 253:520-528.

Motoyama, T., Kojima, N., Horiuchi, H., Ohta, A., and Takagi, M. (1994). Isolation of a chitin synthase gene (chsC) of Aspergillus nidulans. Biosci Biotechnol Biochem 58:2254-2257.

Mouriño-Pérez, R. R., Roberson, R. W., & Bartnicki-García, S. (2006). Microtubule dynamics and organization during hyphal growth and branching in *Neurospora crassa*. Fungal Genet Biol 43:389-400.

Mouriño-Pérez, R.R. (2013). Septum development in filamentous ascomycetes. Fungal Biology Reviews 27:1-9.

Mulholland, J., Preuss, D., Moon, A., Wong, A., Drubin, D. & Botstein, D. (1994). Ultrastructure of the yeast F-actin cytoskeleton and its association with the plasma membrane. J Cell Biol 125:381–391.

Paoletti, A., Chang, F. (2000). Analysis of mid1p, a protein required for placement of the cell division site, reveals a link between the nucleus and the cell surface in fission yeast. Mol. Biol. Cell. 11:2757-2773.

Pelham, R. J., Chang, F. (2001). Role of actin polymerization and actin cables in actin-patch movement in *Schizosaccharomyces pombe*. Nat. Cell Biol. 3:235-244.

Pittenger, M. F., Kazzaz, J. A. & Helfman, D. M. (1994). Functional properties of non-muscle tropomyosin isoforms, Curr. Opin. Cell Biol. 6:96-104.

Plamann, M., Minke, P. F., Tinsley, J. H., & Bruno, K. S. (1994). Cytoplasmic dynein and actin-related protein Arp1 are required for normal nuclear distribution in filamentous fungi. J Cell Biol 127:139-149.

Pollard, T. D. (2008). Progress towards understanding the mechanism of cytokinesis in fission yeast. Biochem Soc Trans 36:425-430.

Pruyne, D., Bretscher, A. (2000). Polarization of cell growth in yeast. J. Cell. Sci. 113 (Pt 4):571-585.

Ramos-García, S. L., Roberson, R. W., Freitag, M., Bartnicki-García, S. & Mouriño-Pérez, R. R. (2009). Cytoplasmic bulk flow propels nuclei in mature hyphae of *Neurospora crassa*. Eukaryotic Cell, *8*(12), 1880-1890.

Rasmussen, C. G., Glass, N. L. (2005). A Rho-Type GTPase, rho-4, Is Required for Septation in *Neurospora crassa*. Eukaryot Cell 4:1913-1925.

Rasmussen, C. G., Glass, N. L. (2007). Localization of RHO-4 indicates differential regulation of conidial versus vegetative septation in the filamentous fungus *Neurospora crassa*. Eukaryot Cell 6:1097-1107.

Riedl, J., Crevenna, A. H., Kessenbrock, K., Yu, J. H., Neukirchen, D., Bista, M., Bradke, F., Jenne, D., Holak, T. A., Werb, Z., Sixt, M. & Wedlich-Söldner, R. (2008). Lifeact:a versatile marker to visualize F-actin. Nat. Methods. 5:605-607.

Riquelme, M., Bartnicki-García, S. (2008). Advances in understanding hyphal morphogenesis:Ontogeny, phylogeny and cellular localization of chitin synthases. Fungal Biol Rev 22:56-70.

Riquelme, M., Bartnicki-García, S., González-Prieto, J. M., Sánchez-León, E. F., Verdín-Ramos, J. A., Beltrán-Aguilar, A., & Freitag, M. (2007). Spitzenkörper localization and intracellular traffic of GFP-labeled CHS-3 and CHS-6 chitin synthases in living hyphae of *Neurospora crassa*. Eukaryot Cell 6:1853-1864.

Riquelme, M., Yarden, O., Bartnicki-Garcia, S., Bowman, B., Castro-Longoria, E., Free, S. J., Fleissner, A., Freitag, M., et al. (2011). Architecture and development of the Neurospora crassa hypha -- a model cell for polarized growth. Fungal Biol 115:446-474.

Roberson, R. W., Abril, M., Blackwell, M., Letcher, P., McLaughlin, D. J., Mouriño-Pérez, R. R., Riquelme, M. & Uchida, M. (2009). Hyphal Structure, Chapter 2. In, Cellular and Molecular Biology of Filamentous Fungi. Eds. Borkovich, K. and Ebbole, D. ASM Press, Washington, D.C.

Roberson, R. W., Fuller, M. S. (1988). Ultrastructural aspects of the hyphal tip of *Sclerotium rolfsii* preserved by freeze substitution. Protoplasma 146:143-149.

Roberson, R.W. (1992). The actin cytoskeleton in hyphal cells of *Sclerotium rolfsii*. Mycologia 84, 41-51.

Rodal, A. A., Kozubowski, L., Goode, B. L., Drubin, D. G. & Hartwig, J. H. (2005). Actin and septin ultrastructures at the budding yeast cell cortex. Mol. Biol. Cell. 16:372-384.

Sambrook, J., Fritsch E. F. & Maniatis T. (1989). Molecular cloning:a laboratory manual. Cold Spring Harbor Laboratory Press, Cold Spring Harbor, NY.

Sánchez-León-Hing, E. F., Verdin-Ramos, J. A., Freitag, M., Roberson R. W., Bartnicki-Garcia, S., & Riquelme, M. (2011). Traffic of chitin synthase 1 (CHS-1) to the Spitzenkörper and developing septa in hyphae of *Neurospora crassa*:Actin dependence and evidence of distinct microvesicle populations. Eukaryot Cell 10:683-695.

Sandrock, T. M., Brower, S. M., Toenjes, K. A. & Adams, A. E. (1999). Suppressor analysis of fimbrin (Sac6p) overexpression in yeast. Genetics. 151:1287-1297.

Seiler, S., Justa-Schuch, D. (2010). Conserved components, but distinct mechanisms for the placement and assembly of the cell division machinery in unicellular and filamentous ascomycetes. Mol Microbiol 78:1058-1076.

Serna, L., Stadler, D. (1978). Nuclear division cycle in germinating conidia of *Neurospora crassa*. J. Bacteriol 136:341-351.

Sharpless, K. E., Harris, S. D. (2002). Functional characterization and localization of the *Aspergillus nidulans* formin SEPA. Mol Biol Cell 13:469-479.

Sheahan, M. B., Staiger, C. J., Rose, R. J. & McCurdy, D.W. (2004). A green fluorescent protein fusion to actin-binding domain 2 of Arabidopsis fimbrin highlights new features of a dynamic actin cytoskeleton in live plant cells. Plant Physiol. 136:3968-3978.

Si, H., Justa-Schuch, D., Seiler, S., & Harris, S. D. (2010). Regulation of septum formation by the Bud3-Rho4 GTPase module in *Aspergillus nidulans*. Genetics 185:165-176.

Smith, M. G., Swamy, S. R., Pon, L. A. (2001). The life cycle of actin patches in mating yeast. J. Cell. Sci. 114:1505-1513.

Sohrmann, M., Fankhauser, C., Brodbeck, C., & Simanis, V. (1996). The dmf1/mid1 gene is essential for correct positioning of the division septum in fission yeast. Genes Dev 10:2707-2719.

Srinivasan, S., Vargas, M. & Roberson, R. W. (1996). Functional, organizational, and biochemical analysis of F-actin in the hyphal tip cells of *Allomyces macrogynus*. Mycologia 88:57-80.

Steyer, J. A., Almers, W. A. (2001). Real-time view of life within 100nm of the plasma membrane. Nat Rev Mol Cell Biol 2:268-276

Taheri-Talesh, N., Horio, T., Araujo-Bazán, L., Dou, X., Espeso, E. A., Peñalva, M.A., Osmani, S. A., & Oakley, B. R. (2008). The tip growth apparatus of *Aspergillus nidulans*. Mol. Biol. Cell. 19:1439-1449.

Takeshita, N., Ohta, A., & Horiuchi, H. (2005). CsmA, a class V chitin synthase with a myosin motor-like domain, is localized through direct interaction with the actin cytoskeleton in *Aspergillus nidulans*. Mol Biol Cell 16:1961-1970.

Takeshita, N., Vienken, K., Rolbetzki, A., & Fischer, R. (2007). The *Aspergillus nidulans* putative kinase, KfsA (kinase for septation), plays a role in septation and is required for efficient asexual spore formation. Fungal Genet Biol 44:1205-1214.

Torralba, S., Raudaskoski, M., Pedregosa, A. M. & Laborda, F. (1998). Effect of cytochalasin A on apical growth, actin cytoskeleton organization and enzyme secretion in *Aspergillus nidulans*. Microbiology. 144 (Pt 1):45-53.

Upadhyay, S., Shaw, B. D. (2008). The role of actin, fimbrin and endocytosis in growth of hyphae in *Aspergillus nidulans*. Mol. Microbiol. 68:690-705.

Vallen, E. A., Caviston, J., & Bi, E. (2000). Roles of Hof1p, Bni1p, Bnr1p, and myo1p in cytokinesis in *Saccharomyces cerevisiae*. Mol Biol Cell 11:593-611.

Vavylonis, D., Wu, J., Hao, S., O'Shaughnessy, B., & Pollard, T. D. (2008). Assembly mechanism of the contractile ring for cytokinesis by fission yeast. Science 319:97-100.

Virag, A., Griffiths, A. J. F. (2004). A mutation in the *Neurospora crassa* actin gene results in multiple defects in tip growth and branching. Fungal Genet. Biol. 41:213-225.

Waddle, J. A., Karpova, T. S., Waterston, R. H. & Cooper, J. A. (1996). Movement of cortical actin patches in yeast. J. Cell Biol. 132:861-870.

Wang, Y., Fan, L. M., Zhang, W. Z., Zhang, W., Wu, W. H. (2004). Ca2+-permeable channels in the plasma membrane of Arabidopsis pollen are regulated by actin microfilaments. Plant Physiol. 136:3892-3904.

Weber, I., Assmann, D., Thines, E., & Steinberg, G. (2006). Polar localizing class V myosin chitin synthases are essential during early plant infection in the plant pathogenic fungus *Ustilago maydis*. Plant Cell 18:225-242.

Wedlich-Soldner, R., Altschuler, S., Wu, L. & Li, R. (2003). Spontaneous Cell Polarization Through Actomyosin-Based Delivery of the Cdc42 GTPase. Science. 299:1231-1235.

White, J. G., Borisy, G. G. (1983). On the mechanisms of cytokinesis in animal cells. J. Theor. Biol. 101:289-316.

Wolkow, T. D., Harris, S. D., & Hamer, J. E. (1996). Cytokinesis in *Aspergillus nidulans* is controlled by cell size, nuclear positioning and mitosis. J Cell Sci 109:2179-2188.

Wong, K. C. Y., D'souza, V. M., Naqvi, N. I., Motegi, F., Mabuchi, I. & Balasubramanian, M. K. (2002). Importance of a myosin II-containing progenitor for actomyosin ring assembly in fission yeast. Curr. Biol. 12:724-729.

Wu, J. Q., Kuhn, J. R., Kovar, D. R., & Pollard, T. D. (2003). Spatial and temporal pathway for assembly and constriction of the contractile ring in fission yeast cytokinesis. Dev Cell 5:723-734.

Wu, J., Kuhn, J. R., Kovar, D. R. & Pollard, T. D. (2003). Spatial and temporal pathway for assembly and constriction of the contractile ring in fission yeast cytokinesis. Dev. Cell. 5:723-734.

Wu, J., Pollard, T. D. (2005). Counting cytokinesis proteins globally and locally in fission yeast. Science. 310:310-314.

Wu, J., Sirotkin, V., Kovar, D. R., Lord, M., Beltzner, C. C., Kuhn, J. R. & Pollard, T. D. (2006). Assembly of the cytokinetic contractile ring from a broad band of nodes in fission yeast. J. Cell Biol. 174:391-402.

Yamada, E., Ichinomiya, M., Ohta, A. & Horiuchi, H. (2005). The class V chitin synthase gene csmA is crucial for the growth of the chsA chsC double mutant in *Aspergillus nidulans*. Biosci Biotechnol Biochem 69:87-97.

Young, M. E., Cooper, J. A. & Bridgman, P. C. (2004). Yeast actin patches are networks of branched actin filaments, J. Cell Biol. 166:629-635.